

**Repository of the Max Delbrück Center for Molecular Medicine (MDC)
in the Helmholtz Association**

<https://edoc.mdc-berlin.de/21160/>

**Combinatorial, additive and dose-dependent drug-microbiome
associations**

Forslund S.K., Chakaroun R., Zimmermann-Kogadeeva M., Markó L., Aron-Wisnewsky J., Nielsen T., Moitinho-Silva L., Schmidt T.S.B., Falony G., Vieira-Silva S., Adriouch S., Alves R.J., Assmann K., Bastard J.P., Birkner T., Caesar R., Chilloux J., Coelho L.P., Fezeu L., Galleron N., Helft G., Isnard R., Ji B., Kuhn M., Le Chatelier E., Myridakis A., Olsson L., Pons N., Prifti E., Quinquis B., Roume H., Salem J.E., Sokolovska N., Tremaroli V., Valles-Colomer M., Lewinter C., Søndertoft N.B., Pedersen H.K., Hansen T.H., Gøtze J.P., Køber L., Vestergaard H., Hansen T., Zucker J.D., Hercberg S., Oppert J.M., Letunic I., Nielsen J., Bäckhed F., Ehrlich S.D., Dumas M.E., Raes J., Pedersen O., Clément K., Stumvoll M., Bork P.

This is the final version of the accepted manuscript. The original article has been published in final edited form in:

Nature
2021 DEC 16 ; 600: 500-505
2021 DEC 08 (first published online: final version)
doi: [10.1038/s41586-021-04177-9](https://doi.org/10.1038/s41586-021-04177-9)

URL: <https://www.nature.com/articles/s41586-021-04177-9>

Publisher: [Springer Nature](#)

Copyright © The Author(s), under exclusive licence to Springer Nature Limited 2021.

Publisher's Notice

This is a post-peer-review, pre-copyedit version of an article published in *Nature*. The final authenticated version is available online at: <https://doi.org/10.1038/s41586-021-04177-9>.

Combinatorial, additive and dose-dependent drug-microbiome associations

Sofia K. Forslund^{1,2,3,4,5,31*}, Rima Chakaroun^{6*}, Maria Zimmermann-Kogadeeva^{1*}, Lajos Markó^{2,4,5*}, Judith Aron-Wisnewsky^{7,8*}, Trine Nielsen^{9*}, Lucas Moitinho-Silva¹, Thomas S. B. Schmidt¹, Gwen Falony¹⁵, Sara Vieira-Silva¹⁵, Solia Adriouch⁷, Renato J. Alves^{1,10}, Karen Assmann⁷, Jean-Philippe Bastard^{11,12}, Till Birkner^{2,3}, Robert Caesar¹³, Julien Chilloux¹⁴, Luis Pedro Coelho¹, Leopold Fezeu¹⁶, Nathalie Galleron¹⁷, Gerard Helft¹⁸, Richard Isnard¹⁸, Boyang Ji¹⁹, Michael Kuhn¹, Emmanuelle Le Chatelier¹⁷, Antonis Myridakis¹⁴, Lisa Olsson¹³, Nicolas Pons¹⁷, Edi Prifti^{7,20,21}, Benoit Quinquis¹⁷, Hugo Roume¹⁷, Joe-Elie Salem²², Nataliya Sokolovska⁷, Valentina Tremaroli¹³, Mireia Valles-Colomer¹⁵, Christian Lewinter²³, Nadja B. Søndertoft⁹, Helle Krogh Pedersen⁹, Tue H. Hansen⁹, The MetaCardis Consortium**, Jens Peter Gøtze²⁴, Lars Køber²³, Henrik Vestergaard^{9,25}, Torben Hansen⁹, Jean-Daniel Zucker^{7,20,21}, Serge Hercberg¹⁶, Jean-Michel Oppert⁸, Ivica Letunic^{1,26}, Jens Nielsen¹⁹, Fredrik Bäckhed^{9,13}, S. Dusko Ehrlich¹⁷, Marc-Emmanuel Dumas^{14,27,28,29}, Jeroen Raes¹⁵, Oluf Pedersen⁹, Karine Clément^{7,8+}, Michael Stumvoll^{6,30+}, Peer Bork^{1,3+}

* contributed equally

+ corresponding authors

E-mail: KC (karine.clement@inserm.fr) MS (michael.stumvoll@medizin.uni-leipzig.de) PB (peer.bork@embl.org)

** MetaCardis Consortium Collaborators

Chloe Amouyal, Ehm Astrid Andersson Galijatovic, Fabrizio Andreelli, Olivier Barthelemy, Jean-Paul Batisse, Eugeni Belda, Magalie Berland, Randa Bittar, Hervé Blottière, Frederic Bosquet, Rachid Boubrit, Olivier Bourron, Mickael Camus, Dominique Cassuto, Cecile Ciangura, Jean-Philippe Collet, Maria-Carlota Dao, Morad Djebbar, Angélique Doré, Line Engelbrechtsen, Soraya Fellahi, Sebastien Fromentin, Pilar Galan, Dominique Gauguier, Philippe Giral, Agnes Hartemann, Bolette Hartmann, Jens Juul Holst, Malene Hornbak, Lesley Hoyles, Jean-Sebastien Hulot, Sophie Jacqueminet, Niklas Rye Jørgensen, Hanna Julienne, Johanne Justesen, Judith Kammer, Nikolaj Karup, Mathieu Kerneis, Jean Khemis, Ruby Kozlowski, Véronique Lejard, Florence Levenez, Lea Lucas-Martini, Robin Massey, Laura Martinez-Gili, Nicolas Maziers, Jonathan Medina-Stamminger, Gilles Montalescot, Sandrine Moutel, Ana Luisa Neves, Michael Olanipekun, Laetitia Pasero Le Pavin, Christine Poitou, Françoise Pousset, Laurence Pouzoulet, Andrea Rodriguez-Martinez, Christine Rouault, Johanne Silvain, Mathilde Svendstrup, Timothy D. Swartz, Thierry Vanduyvenboden, Camille Vatier, Stefanie Walther.

Author Affiliations:

1 Structural and Computational Biology Unit, European Molecular Biology Laboratory, Heidelberg, Germany

2 Experimental and Clinical Research Center, a cooperation of Charité-Universitätsmedizin and the Max-Delbrück Center, Berlin, Germany

3 Max Delbrück Center for Molecular Medicine (MDC), Berlin, Germany

4 Charité – Universitätsmedizin Berlin, Berlin, Germany

5 Berlin Institute of Health (BIH), Berlin, Germany

6 Medical Department III - Endocrinology, Nephrology, Rheumatology, University of Leipzig Medical Center, Leipzig, Germany

7 Sorbonne Université, INSERM, Nutrition and obesities; systemic approaches (NutriOmics), Paris, France

8 Assistance Publique Hôpitaux de Paris, Pitie-Salpêtrière Hospital, Nutrition department, Paris, France

9 Novo Nordisk Foundation Center for Basic Metabolic Research, Faculty of Health and Medical Sciences, University of Copenhagen, Copenhagen, Denmark

10 Collaboration for joint PhD degree between EMBL and Heidelberg University, Faculty of Biosciences, Heidelberg, Germany

11 Assistance Publique Hôpitaux de Paris, UF Biomarqueurs Inflammatoires et Métaboliques, Biochemistry and Hormonology Department, Tenon Hospital, Paris, France

12 Sorbonne Université-INSERM UMR S_938, Centre de Recherche Saint-Antoine, Paris, France

13 Wallenberg Laboratory, Department of Molecular and Clinical Medicine and Sahlgrenska Center for Cardiovascular and Metabolic Research, University of Gothenburg, Gothenburg, Sweden

14 Division of Systems Medicine, Department of Metabolism, Digestion and Reproduction, Faculty of Medicine, Imperial College London, London, United Kingdom

15 Center for Microbiology, VIB, KU Leuven, University of Leuven, Leuven, Belgium

16 Sorbonne Paris Cité Epidemiology and Statistics Research Centre (CRESS), U1153 Inserm, U1125, Inra, Cnam, University of Paris 13, Nutritional Epidemiology Research Team (EREN), 93017, Bobigny, France

- 17 Metagenopolis, INRA, AgroParisTech, Université Paris-Saclay, France
- 18 Assistance Publique Hôpitaux de Paris, Pitié-Salpêtrière Hospital, Cardiology department, Paris, France
- 19 Department of Biology and Biological Engineering, Chalmers University of Technology, Gothenburg, Sweden
- 20 Institute of Cardiometabolism and Nutrition, Integromics Unit, Paris, France
- 21 Sorbonne Université, IRD, Unité de Modélisation Mathématique et Informatique des Systèmes Complexes, UMMISCO, Bondy, France
- 22 Assistance Publique Hôpitaux de Paris, Pitié-Salpêtrière Hospital, Department of Pharmacology, UNICO Cardio-oncology Program, CIC-1421; INSERM, Sorbonne Université, Paris, France.
- 23 Department of Cardiology, Rigshospitalet, University of Copenhagen, Copenhagen, Denmark
- 24 Department of Clinical Biochemistry, Rigshospitalet, University of Copenhagen, Copenhagen, Denmark
- 25 Department of Medicine, Bornholms Hospital, Rønne, Denmark
- 26 Biobyte Solutions GmbH, Heidelberg, Germany
- 27 Genomic and Environmental Medicine, National Heart & Lung Institute, Faculty of Medicine, Imperial College London, London, United Kingdom
- 28 European Genomic Institute for Diabetes, CNRS UMR 8199, INSERM UMR 1283, Institut Pasteur de Lille, Lille University Hospital, University of Lille, Lille, France
- 29 McGill University and Genome Quebec Innovation Centre, Montréal, QC, Canada
- 30 Helmholtz Institute for Metabolic, Obesity and Vascular Research (HI-MAG) of the Helmholtz Zentrum München at the University of Leipzig, Leipzig, Germany
- 31 DZHK (German Centre for Cardiovascular Research), partner site Berlin, Berlin, Germany

Upon transition from health to cardiometabolic disease (CMD), patients are heavily medicated, leading to increasingly aberrant gut microbiome and serum metabolome and complicating quests for biomarkers¹⁻⁵. Through integrated multi-omics analyses of 2,173 European residents (MetaCardis cohort), we show that the explanatory power of drugs for variability of both host and gut microbiome features exceeds that of disease. We quantify inferred effects of single and combinatorial medications as well as additive effects, shifting metabolome and microbiome towards a healthier state, such as synergistic reduction of serum atherogenic lipoproteins by statins combined with aspirin, or enrichment of intestinal *Roseburia* by diuretics combined with beta-blockers. Several antibiotics exhibit quantitative relationship between number of courses prescribed and progression towards a microbiome state associated with CMD severity. We further report a relationship between cardiometabolic drug dosage, improvement in clinical markers, and microbiome composition, supporting direct drug effects. Taken together, our computational framework and resulting resources allow disentangling drug from disease effects on host and microbiome features in multi-medicated subjects. Furthermore, the robust signatures identified with our framework provide new hypotheses for drug-host-microbiome interactions in cardiometabolic disease.

Identifying robust gut microbiota contributions to health and disease requires complex technical and statistical frameworks^{1,2} and remains challenging due to many covariates affecting both microbial composition³⁻⁵ and disease. Common covariates are therapeutic drugs^{4,6-10}, such as broadly prescribed proton pump inhibitors (PPIs)⁶ and type 2 diabetes (T2D) drug metformin⁷, which impact the gut microbiota and modulate inflammation¹¹. Furthermore, direct drug-microbial interactions have been demonstrated *in vitro*⁸. For several drugs in a mostly healthy population, their usage explained more variance in microbiota composition than other covariates tested, albeit with small individual effect sizes¹². However, studies in healthy populations^{12,13} are inadequate for investigating the secondary impacts of drugs in the context of chronic diseases. To robustly disentangle drug-microbiome associations from host and disease factors, large sample sizes and high resolution of clinical phenotypes and medication are required, while accounting for known variables affecting the gut microbiome.

Finally, drug effects are often dose-dependent, yet dosage is rarely considered in microbiome studies.

To overcome these limitations, we propose a general framework for separating disease from treatment associations in multi-omics cross-sectional studies and apply it to gut metagenomic, host clinical and metabolomic measurements of 2,173 European residents from the multi-centre MetaCardis cohort. MetaCardis includes patients with metabolic syndrome (MetS), severe and morbid obesity, T2D, acute and chronic coronary artery disease (CAD), and heart failure (HF), and healthy controls. Considering CMD- and other frequently prescribed medications, we investigated drug-host-microbiome associations for eight major indications (antidiabetic, antihypertensive, antidyslipidemic, antithrombotic, antiarrhythmic agents, gout medication, PPIs, and antibiotics). The most commonly prescribed CMD drugs were statins (n = 772, 35.5%), beta-blockers (n = 656, 30.2%), metformin (n = 607, 27.9%), aspirin (n = 532, 24.5%), angiotensin converting enzyme (ACE) inhibitors (n = 470, 21.6%) and angiotensin II receptor blockers (ARB) (n = 470, 21.6%), often taken in combination (Supplementary Tables 1-4). We therefore studied individual drug effects, and their synergistic and additive interactions in the context of available phenotypic, dietary, and demographic variables, molecular readouts including serum concentrations of lipoproteins, cytokines and metabolites, and taxonomic and functional profiles of the gut microbiome.

To quantify the overall impact of medications, we performed multivariate regression of explained variance of host and microbiome data onto total influence of medications, clinical and environmental factors, and disease status. All drugs together explain more variation in the microbiome composition than disease group alone, or any other factor considered under a conservative estimate. However, in line with previously reported high individual variability¹⁴, only 1.7 - 9% of variation between subjects is explainable by factors included in the model, of which 1 - 2.5% are attributable to drug intake, comparable to disease status, diet and smoking combined (Figure 1a, Supplementary Table 5).

To quantify individual drug effects, we implemented a univariate statistical approach to disentangle drugs from disease associations with the gut microbiome and host features. Thus, features distinguishing patient groups from healthy controls are divided into i) confidently deconfounded features of CMD, ii) ambiguously deconfounded (where both treatment and disease strongly correlate), and iii) confounded (unambiguous drug associations) (Extended Data Figure 1). A major fraction of naïve associations (e.g.

45% for T2D) between drugs and microbiome or metabolome is attributable to drug intake (Figure 1b, Supplementary Table 5). Nonetheless, we recover previously described metabolic disease signatures and show that these cannot be reduced to treatment effects (Extended Data Figure 2, Supplementary Results). We thus conclude that a drug-conscious approach uncovers true disease associations and is crucial to circumvent highly inflated treatment-confounded false positives in biomarker discovery.

Next, we disentangled potential direct effects of the medication (where treatment association direction opposes the disease association) from potential severity markers (concordant direction of the treatment and disease association). Of 28 cardiometabolic drugs taken by at least 10 individuals within at least one patient group, the strongest effects on serum metabolome were found for antidiabetic drugs, statins, beta-blockers, antithrombotic drugs and aspirin. While drugs with the same indication (i.e. antidiabetic, antihypertensive) had concordant associations with host features, the impact on the gut microbiome was more diverse in effect size and direction between these drugs (Figure 1c, Supplementary Tables 6, 7). Our approach recaptured previously reported findings on the impact of antibiotics¹⁵, PPIs^{16,17}, statins¹¹, beta-blockers and metformin^{7,18} (Extended Data Figure 3). More importantly, we identified novel associations for these as well as for other highly prevalent drugs (Supplementary Results). For example, we identified aspirin-associated changes in microbial species abundances, and shifts in serum lipidome and metabolome associated with improved cardiometabolic health (e.g. depletion of *Ruminococcus gnavus*, *Clostridium glycyrrhizinilyticum* and *Parvimonas micra*, reduction of plasma concentrations of inflammatory markers (CRP and IL6), decreased levels of pyruvate, glutamate and succinate at comparable significance to that of the aspirin levels detected in serum of medicated subjects; Figure 1d). In addition, γ -butyrobetaine, a recently identified proatherogenic intermediate of microbial metabolism¹⁹, is lower in subjects taking aspirin, revealing a potential complex antiatherogenic effect of the drug beyond its known platelet-inhibitory functions²⁰. For metformin, we deduce novel antidiabetic effects possibly related to lowered glutamate levels²¹ ($d = -0.17$, FDR = 0.02), due to reduced microbial glutamate transport ($d = -0.2$, FDR = 0.006), along with increased microbial vitamin B12 uptake ($d = 0.32$, FDR=3.65e-6), potentially causing vitamin B12 deficiency in the host, a known metformin side effect (Supplementary Results, Supplementary Table 6). PPIs had the most associations with the gut microbiome features (Figure 1c, Supplementary Table 7) including higher prevalence of presumably

oral bacteria, supporting the hypothesized PPI-caused transfer of oral bacteria into the gut upon decreased stomach acidity¹⁷. Single nucleotide variation (SNV) analysis based on large reference cohorts revealed increased abundance of oral-based strains of *Rothia*, *Haemophilus* and *Streptococcus* species in the gut of subjects taking PPIs, implying that the patient's own oral strains colonize the intestine as gastric acidity weakens²² (Extended Data Figure 4, Supplementary Results).

Beyond single drugs, MetaCardis enables analysis of combinatorial (polypharmacy) effects, since 1,300 individuals were prescribed more than one drug (average intake of 3 drugs with some receiving up to 13 distinct drugs per day) (Figure 2a, b, Supplementary Tables 2, 3). Polypharmacy in CMD mostly reflects concurrence of metabolic diseases, risk factors, or treatments preventing the recurrence of an atherosclerotic event, but also includes medications co-prescribed to reduce side effects, such as PPIs with aspirin to prevent gastric ulcers and bleeding. Multi-medicated patients often exhibit a more pronounced improvement in disease markers than those receiving either drug alone, consistent with synergistic interactions between drugs. In the T2D group, the most pronounced synergistic effects on the microbiome features were observed for loop diuretics, especially in combination with aspirin, ACE-inhibitors and beta-blockers, whereas the most pronounced synergistic effects on host features were observed for statins (Figure 2c). For example, loop diuretics combined with aspirin, ACE-inhibitors or beta-blockers more strongly enrich microbiome-related health markers²³ including *Roseburia* abundance¹¹ (combination: $d = 0.46$, $d = 0.51$, $d = 0.36$, correspondingly, single drugs: diuretics $d = 0.27$). Taken with metformin or aspirin, statins are associated with lower intermediate-, low-, and very low-density lipoprotein (IDL, LDL and vLDL) levels in serum and total body fat mass, while increasing microbiome richness and abundance of Firmicutes and methanogenic bacteria depleted in the T2D group (Figure 2d, Supplementary Tables 8, 9). These shifts in the microbiome might mediate some of the synergistic drug effects on the host (Figure 2e, Supplementary Table 10, Supplementary Results).

Next, we investigated additive drug associations. The strongest of those we observed for antibiotics using five-year retrospective exposure (total number of courses). Antibiotics are frequently prescribed in CMD due to an increased prevalence of infections²⁴. Yet, epidemiological studies link antibiotics with an increased risk for obesity, T2D, metabolic and inflammatory diseases²⁵. Previous antibiotic exposure is significantly (i) associated with lower gut gene richness within the same subject groups (Figure 3a,

Spearman rho = -0.25, $P = 3.7e-5$) and, (ii) correlated with total abundance of antimicrobial resistance genes (AMR) in the gut (controls: Spearman rho = 0.30, $P = 9e-7$; T2D subjects: Spearman rho = 0.20, $P = 2e-5$) (Figure 3b). These findings imply cumulative, additive shifts upon repeated antibiotic exposure towards a more resistant but less diverse microbiota, which is a hallmark of microbiome signature in obesity, insulin resistance and low-grade inflammation²⁶. The same properties distinguish antibiotics-naïve CMD patients from healthy controls confirming an impact of repeated antibiotic exposures (antibiotics-naïve healthy vs T2D richness two-sided MWU test $P = 7.9e-21$; AMR gene abundance $P = 2e-2$). Using principal component analysis (PCA, Supplementary Table 11), we show that the first PC of microbiome composition, explaining 45% of variation and correlating with gene richness, is associated both with an additive effect of antibiotics and metabolic impairment following antibiotics exposure (antibiotic effect: controls: Spearman rho = 0.27, $P = 1.7e-5$; T2D subjects: Spearman rho = 0.16, $P = 7e-4$; antibiotics-naïve vs antibiotics treated healthy (two-sided MWU test $P = 1e-3$) and T2D subjects ($P = 1e-3$)) (Figure 3c). Multivariate breakdown of these shifts reveals reduced abundance of *Prevotella copri* and *Faecalibacterium prausnitzii*, and an increase in *Bacteroides vulgatus* and *Bacteroides dorei*, abundant genera constituting hallmarks of enterotypes^{27,28}. Further, we show that shifts in gut microbial metabolic functions link additive effects of specific antibiotics groups to CMD susceptibility (Extended Data Figures 5-7, Supplementary Table 12, Supplementary Results).

Furthermore, the detailed medication tracking in MetaCardis allows to investigate the effect of dosage on the host and microbiota. For the 20 drugs with sufficient dosage information, we distinguished between dosage-confirmed effects, i.e., features significantly associated both with drug intake and with its dosage; and dosage-unique effects, where dosage analysis revealed associations not captured by other analyses. The drugs with the most features confirmed by dosage analysis were metformin, sulfonylurea, insulin, PPI, gout medications, and statins; whereas the most dosage-unique associations were reported for metformin and statins (Figure 3d). Statin dosage was negatively associated with atherogenic vLDL levels, highlighting the intended dose-dependent lipid lowering effects, and positively associated with health-promoting *Roseburia* species in the gut¹¹. Metformin dosage was negatively associated with cytokine levels (SDF1 and MIF), consistent with previous reports of its anti-inflammatory effects^{29,30}. Furthermore, we observed a shift between Bact1 and Bact2 enterotypes in patients taking higher dosages

of metformin, the latter also associated with disease, proposing Bact2 enterotype as a severity marker in T2D (Figure 3e, f, Supplementary Tables 13, 14). For statins, dosage analysis strengthens the reported observation of microbiome shifts towards a healthier state away from Bact2 enterotype¹¹. Moreover, dosage analysis uniquely identified Bact2 and Prev enterotypes as severity markers for beta-blocker usage in individuals with severe and morbid obesity (Figure 3e, f, Supplementary Table 14).

With stringent analytical approaches, we show that not only medication intake, but also dosage, drug combinations and previous exposure to antibiotics should be captured in human studies to disentangle the drug-host-microbiome interactions in complex diseases. For several drugs, our results identify microbiome shifts associated with medication intake, which might mediate the improvement in clinical markers. Given the observational study design, our analysis enables the identification of associative (and not necessarily causative) effects of drugs on variations in the microbiome and clinical phenotypes. Thus, experimental validation in animal models (e.g. multimodal effect of low-dose aspirin or synergistic effects of statin and aspirin or metformin in high-fat fed LDL-receptor-deficient mice) is required to substantiate these findings, since controlled clinical trials can be challenging in a population with multimorbidity. Disentangling medication effects on the gut microbiome and serum metabolome, as illustrated here, is the first step towards understanding the systemic effects of drugs at the molecular level, while pre-clinical tests should be performed to assess their significance in terms of health outcomes for CMD. To improve treatment in the context of genetic and microbiome variability and complex drug regimens, robust molecular markers are needed to identify the transition from health to chronic diseases. Subsequently, the gut modulation potential of drugs could be harnessed to reverse disease progression in a personalized manner.

Figures

Figure 1.

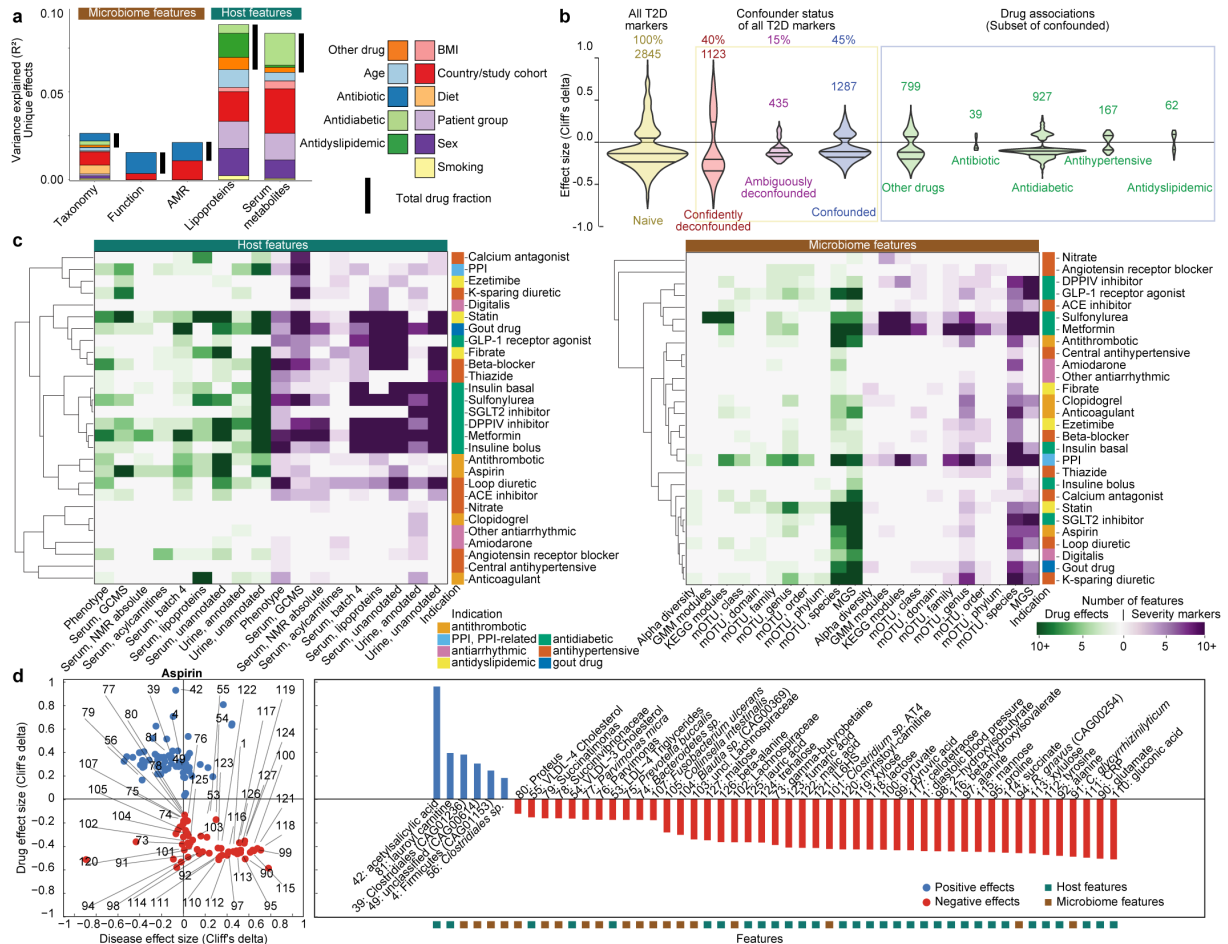


Figure 1. Associations between CMD drugs, host and microbiome.

a. Stacked bar charts show variance explained (R^2) by variable group and feature type.

b. Confounder analysis of features differentially abundant between T2D and control subjects; violins represent distribution of effect size, number of features per category listed. “Naïve associations” (yellow, two-sided MWU FDR < 0.1) are either confounded or ambiguously/confidently deconfounded (blue, purple and red violins). Green violins show breakdown of confounders by drug category.

c. Hierarchical clustering of host (left) and microbiome (right) features associated with each drug in at least one patient group. Features separate into potential drug effects (discordant with disease associations) and severity markers (concordant with disease associations).

d. Scatterplot (left) shows effect sizes (Cliff's delta) of confidently deconfounded associations between aspirin usage and features versus disease effect size within each clinical group. A subset of features is highlighted for interpretation (right).

Figure 2.

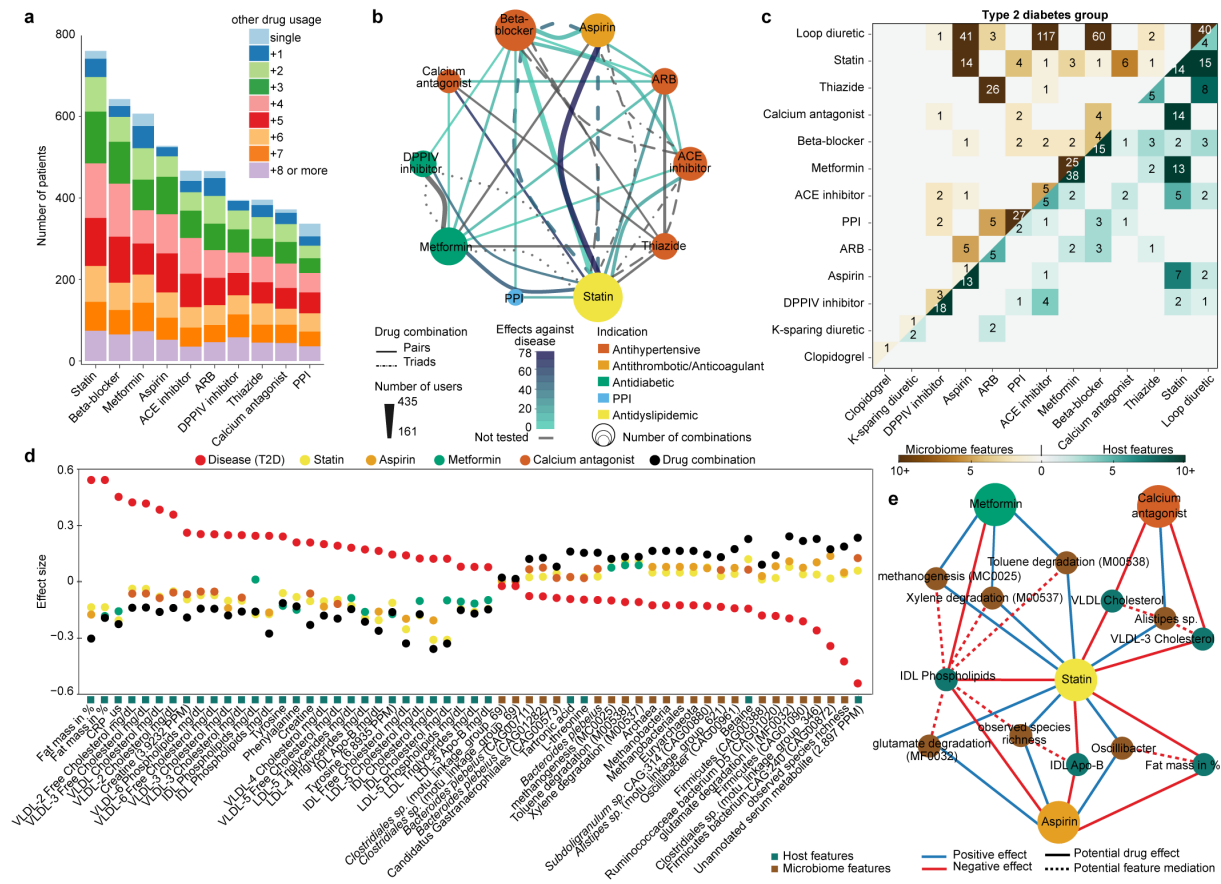


Figure 2. Combinatorial impacts of CMD drugs.

- a. Number of CMD patients receiving each drug in combination with a specified number of other drugs.
- b. The thirty most common drug combinations represented as a graph. Node size is proportional to the number of combinations; edge width is proportional to the number of users per combination; color corresponds to the number of significant drug associations. Solid lines: drug pairs; dotted/dashed lines: drug triplets.
- c. Heatmap shows number of features (host (bottom, green) and microbiome (top, brown)) affected by each drug combination more strongly than by single drugs among T2D patients. Diagonal values show number of features affected by each drug alone.

d. Effect size (Cliff's delta) of disease associations (red), drug combinations (black), and single drugs (other colors) among T2D patients for the combination of statin and metformin, aspirin, or calcium antagonist. Each item on the horizontal axis corresponds to a drug combination-feature association.

e. Drug-feature graph showing potential mediation between host and microbiome features. Solid line color represents direction of drug effect. Dashed line color represents the sign of Pearson's correlation coefficient ($P < 0.1$) between potentially mediated features (Supplementary Tables 8, 10).

Figure 3.

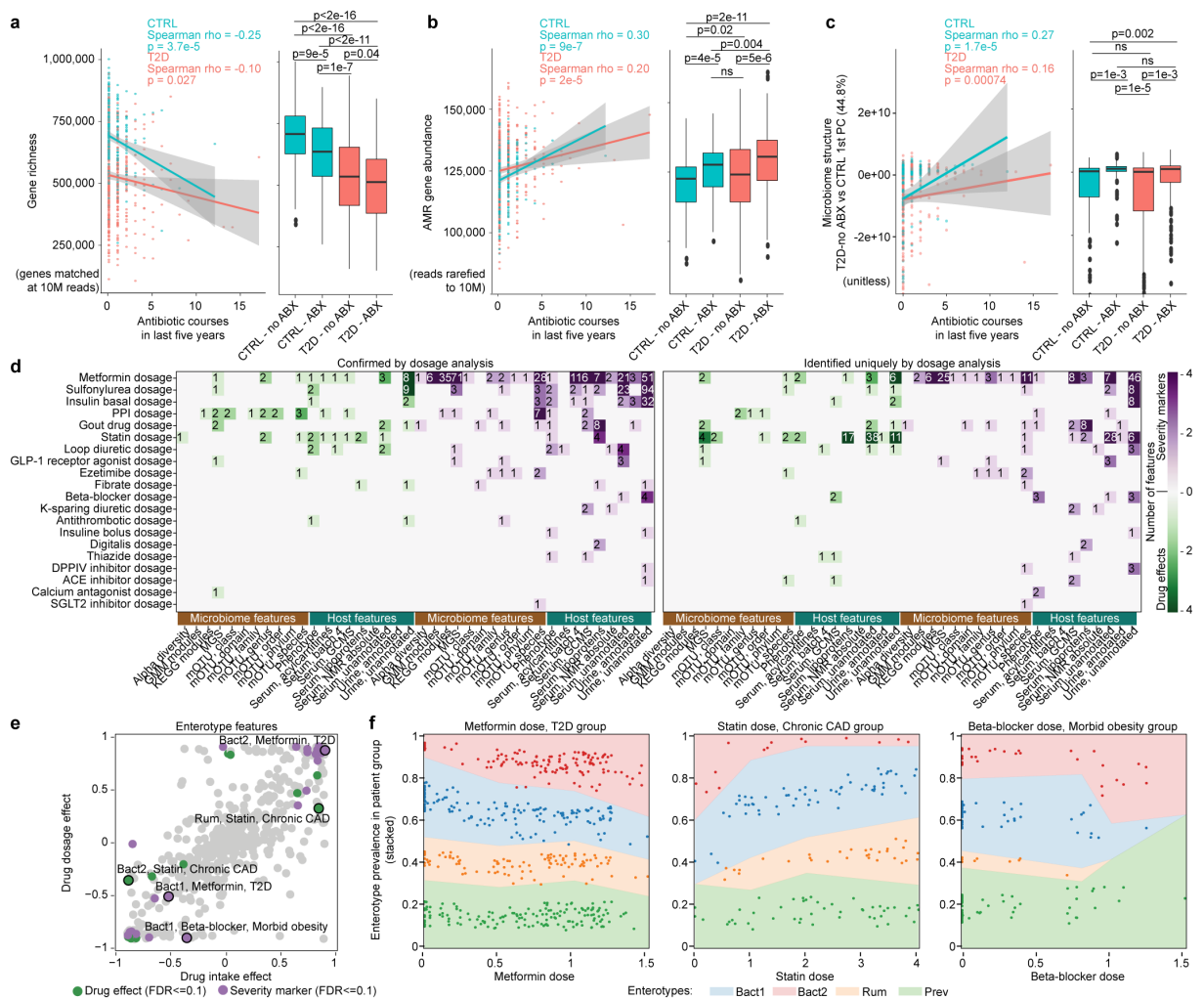


Figure 3. Additive and dose-dependent drug associations with host and microbiome.

Scatterplots show microbiome features (**a**. Gene richness; **b**. Total abundance of AMR; **c**. The first principal component of gut species composition) significantly associated with the number of antibiotics courses in the last 5 years in control (N = 256) and T2D (N = 456) subjects (gray area: 95% CI for linear regression). Boxplots (box showing median and quartiles, whiskers 1.5 interquartile range, dots outliers)

show the comparisons in antibiotics-naïve (N = 148 CTRL, N = 274 T2D) and antibiotics-exposed (N = 108 CTRL, N = 182 T2D) controls and T2D subjects, respectively, with pairwise significances (two-sided MWU tests, FDR-adjusted) shown in figure.

d. Heatmaps show the number of drug-feature associations confirmed by dosage analysis (left), or uniquely revealed by dosage analysis (right). Features are separated by potential drug effects (discordant with the disease effect) or severity markers (concordant with the disease effect).

e. Scatterplot shows relationship between drug intake effect size (Cliff's delta) and drug dosage effect size (Spearman's rho) on enterotype distribution within each patient group. Features significantly affected in either analysis (two-sided, MWU FDR < 0.1) are shown in green (potential drug effects) or purple (potential severity markers). Black circles highlight associations that are depicted in panel f.

Bact1, 2: Bacteroides 1, 2, Prev: Prevotella, Rum: Ruminococcus.

f. Colored areas represent the stacked enterotype prevalence along the drug dosage axis. Each dot represents a patient taking specific drug dose and classified into one of the four enterotypes. Random noise was added for better visualization (Supplementary Tables 11-14).

Methods

Study cohort and sample acquisition

The prospective cross-sectional multi-center study MetaCardis covered a wide range of metabolic and cardiac phenotypes. For the purpose of the study a total of 2,173 subjects including healthy as well as subjects with increasingly severe metabolic and cardiac disease were recruited into eight study groups in Denmark, Germany and France (Supplementary Table 1). Subjects were evaluated for suitability according to standardized inclusion and exclusion criteria across the three sites. Exclusion criteria included past history of abdominal malignancy / intestinal resection / radiation, chronic or acute inflammatory disease, autoimmune disease, history of organ transplantation with immunosuppressive drug intake, severe kidney disease as defined by $eGFR < 50 \text{ ml/min.1.73m}^2$, specific exclusion criteria allowed for a group-dependent specific phenotype acquisition. The study complied with all relevant

international and respective local regulations and aligned with the declaration of Helsinki. The study protocol was approved by the Ethics Committee at the Medical Faculty at the University of Leipzig (application number: 047-13-28012013), the ethical committees of the Capital Region of Denmark (H-3-2013-145) and the ethics committee 'Comite de Protection des Personnes' (CPP) Ile de France III n° IDRCB2013-A00189-36. The study protocol was registered at clinicaltrial.gov (NCT02059538). All participants provided written informed consent.

Groups were defined along international definitions of disease, with obesity defined according to the WHO criteria³³, metabolic syndrome according to the International Diabetes Federation³⁴, T2D by the American Diabetes Association³⁵ and hypertension according to the American College of Cardiology and American Heart Association³⁶. For obesity specifically, subjects were recruited into two groups: group 2a consisting of subjects with mostly severe obesity (referred to in text as 2a: severe obesity), none of whom had T2D or prior cardiovascular conditions, whereas group 2b consisted of mostly subjects with morbid obesity, who were eligible for bariatric surgery (referred to in text as 2b: morbid obesity). T2D was not an exclusion criterion for this particular group (as compared to group 2a) and patients had overall more severe metabolic impairment (Supplementary Table 1). Subjects with heart failure were defined according to the American College of Cardiology, American Heart Association and the Heart Failure Society of America³⁷.

Phenotyping was performed according to standardized operational procedures between countries and included biological samples acquisition and anthropometrics such as weight, height, body mass index calculation (BMI), blood pressure measurement, and body composition analyses using bioimpedance analysis as well as waist and hip circumference measurements.

Participants answered questionnaires related to medical and family history, physical activity, quality of life, eating behavior as well as food intake using a customized validated food frequency questionnaire³⁸. Medication/drug intake was assessed either by direct recall or by medication list when provided, and subjects were questioned on adherence to medication plan by an experienced clinician. Five-year antibiotics intake was assessed by recall in France and Denmark, whereas participants in Germany were requested to provide medication anamnesis from their general practitioners or physicians they were prescribed medications by in the last 5 years.

Cardiometabolic drugs were classified according to indication/category and further subdivided by drug class (Supplementary Table 4), aiming to resolve major mechanisms of action at a granularity allowing for statistical testing. All medication data was curated jointly by the study physicians at each center so as to harmonize representation.

Blood samples were collected via standard venipuncture after an overnight fast and were used to assess metabolic markers in local routine laboratories. Analyses of adipokines, measures of insulin and C-peptide, inflammatory markers, free fatty acids and metabolomics were centralized at Pitié-Salpêtrière hospital. Plasma and serum samples were stored at the respective clinical centers at $-80\text{ }^{\circ}\text{C}$ until shipment to central measuring facility. Stool samples were obtained by each subject at home and were immediately frozen. Frozen samples were then delivered to the respective study centers within 48 h on dry ice and were stored immediately at $-80\text{ }^{\circ}\text{C}$ until analysis. Fasting plasma glucose, total and HDL cholesterol, triglycerides, creatinine and HbA1c levels were measured using enzymatic methods in local laboratories in each center according to benchmarked standardized methods. LDL-Cholesterol concentrations were measured enzymatically for German participants, and values for French and Danish participants were calculated based on the Friedwald equation. Kinetic assays based on coupled enzyme systems were used to measure alanine aminotransferase (ALAT), aspartate aminotransferase (ASAT), and γ -glutamyltransferase (GGT) levels. Ultrasensitive C-reactive protein (usCRP) was measured using an Image Automatic Immunoassay System (Beckman Coulter). High-sensitivity IL-6 was measured using the Human IL-6 Quantikine HD ELISA Kit (R&D Systems). IFN- γ -induced protein 10 (IP-10) and C-X-X motif chemokine ligand 5 (CXCL5), CCL2, Eotaxin, IL7, MIF, MIP1b, SDF1 and VEGFa were measured using a Luminex assay (ProcartaPlex Mix&Match Human 13-plex; eBioscience, San Diego, CA, USA).

Data acquisition and pre-processing

Total faecal DNA from 1,901 subjects was extracted following the International Human Microbiome Standards (IHMS) guidelines (SOP 07 V2 H) and sequenced using ion-proton technology (ThermoFisher Scientific) resulting in 23.3 ± 4.0 million (mean \pm SD) 150-bp single-end reads per sample on average. Reads were cleaned using Alien Trimmer (v0.2.4)³⁹ in order to remove resilient

sequencing adapters and to trim low-quality nucleotides at the 3' side (quality and length cut-off of 20 and 45 bp, respectively). Cleaned reads were subsequently filtered from human and potential food contaminant DNA (using human genome RCh37-p10, *Bos taurus* and *Arabidopsis thaliana* with an identity score threshold of 97%).

Gene abundance profiling was performed using the 9.9 million gene integrated reference catalogue of the human microbiome⁴⁰. Filtered high-quality reads were mapped with an identity threshold of 95% to the 9.9 million-gene catalogue using Bowtie (v2.2.6) included in the METEOR (v3.2) software⁴¹. A gene abundance table was generated by means of a two-step procedure using METEOR. First, the uniquely mapping reads (reads mapping to a single gene in the catalogue) were attributed to their corresponding genes. Second, shared reads (reads that mapped with the same alignment score to multiple genes) were attributed according to the ratio of their unique mapping counts. The gene abundance table was processed for rarefaction and normalization and further analysis using the MetaOMineR⁴² (v1.2) R package. To decrease technical bias due to different sequencing depth and avoid any artefacts of sample size on low abundance genes, read counts were rarefied. The gene abundance table was rarefied to 10 million reads per sample by random sampling of 10 million mapped reads without replacement. The resulting rarefied gene abundance table was normalized according to the FPKM strategy (normalization by the gene size and the number of total mapped reads reported in frequency) to give the gene abundance profile table. Metagenomic species (MGS; co-abundant gene groups with more than 500 genes corresponding to microbial species; n=1,436) were clustered from 1,267 human gut metagenomes used to construct the 9.9 million-gene catalogue⁴³. MGS abundances were estimated as the mean abundance of the 50 genes defining a robust centroid of the cluster (if more than 10% of these genes gave positive signals). MGS taxonomical annotation was performed using all genes by sequence similarity using NCBI blastN; a species-level assignment was given if > 50% of the genes matched the same reference genome of the NCBI database (November 2016 version) at a threshold of 95% of identity and 90% of gene length coverage. Remaining MGS were assigned to a given taxonomical level from genus to superkingdom if more than 50% of their genes had the same level of assignment. Microbial gene richness (gene count) was calculated by counting the number of genes that were detected at least once in a given sample, using the average number of genes counted in ten independent rarefaction

experiments. Moreover, a second approach was used to quantify microbial taxa based on the mOTU approach⁴⁴. The quantification of mOTU abundance per metagenome was performed following the original methodology: (1) short reads were mapped to the database of single-copy marker genes⁴⁴; (2) gene-level abundance tables were computed, normalizing by the size of each gene and the number of input reads, emulating the scaled mode in MOCAT2⁴⁵; (3) within each metagenome, the abundance of all reads mapping to genes within the same mOTU cluster and the same orthologous group (COG), was added together to obtain a mOTU-COG abundance table, emulating the functional mapping of MOCAT2⁴⁵ (which could not be used directly as the file formats were not appropriate); (4) this abundance table was then run through the final step in the NGLess interface⁴⁶ (v1.3.0) to the mOTU tool to obtain the mOTU abundance table (briefly, the abundance of a mOTU is defined as the mean of its constituent COGs, while ignoring non-detected COGs, provided that at least two COGs have been detected, as in the original publication). For quantification of functional modules, metagenome reads mapped to the IGC gene catalog after rarefaction to 10 million reads per sample were binned by functional category, as per the annotations of the previously carried out analysis within the MOCAT2 framework⁴⁵. Functional potentials at each class of annotations (e.g., KEGG modules) were summed within each annotation term.

Determination of faecal microbial load

Microbial loads of faecal samples were determined as described previously⁵³. Briefly, 0.2 g frozen (-80° C) aliquots were dissolved in physiological solution (9 g/L NaCl; Baxter S.A., Belgium) to a total volume of 100 mL (8.5 g/L NaCl; VWR International, Germany). Subsequently, the slurry was diluted 1,000 times. Samples were filtered using a sterile syringe filter (pore size of 5 µm; Sartorius Stedim Biotech GmbH, Germany). Next, 1 mL of the microbial cell suspension obtained was stained with 1 µL SYBR Green I (1:100 dilution in DMSO; shaded 15 min incubation at 37° C; 10,000 concentrate, Thermo Fisher Scientific, Massachusetts, USA). The flow cytometry analysis was performed using a C6 Accuri flow cytometer (BD Biosciences, New Jersey, USA)⁵⁴. Fluorescence events were monitored using the FL1 533/30 nm and FL3 > 670 nm optical detectors. In addition, also forward and sideward-scattered light was collected. The BD Accuri CFlow (v1.0.264.21) software was used to gate and

separate the microbial fluorescence events on the FL1/FL3 density plot from the faecal sample background. A threshold value of 2,000 was applied on the FL1 channel. The gated fluorescence events were evaluated on the forward/sideward density plot, as to exclude remaining background events. Instrument and gating settings were kept identical for all samples (fixed staining/gating strategy³²; Extended Data Figure 8). Based on the exact weight of the aliquots analyzed, cell counts were converted to microbial loads per gram of faecal material.

Quantitative microbiome profiling (QMP)

Phylogenetic quantitative microbiome profiles were built using a modified version of the pipeline described in Vandeputte et al⁴⁷ (<https://github.com/raeslab/QMP/>). In short, sample abundance profiles were downsized to even sampling depth, defined as the ratio between the sample's sampling size (microbial cells sequenced) and microbial load (total microbial cell count). While in 16S amplicon sequencing, sampling size is defined as total sequencing depth, for shotgun metagenomics, it is defined as the average mOTU marker genes coverage⁴⁵. For both, microbial load is determined by flow cytometry as the average total cell count per gram of frozen faecal material. The sequencing depth of each sample was rarefied to the level necessary to equate the minimum observed sampling depth in the cohort. The rarefied mOTU abundance matrix was converted into numbers of cells per gram and quantitative microbiome profiling matrices created for phylum to species levels. Functional quantitative microbiome profiles and quantitative coabundance gene groups⁴³ profiles were constructed by multiplication of relative proportions to an indexing factor proportional to the microbial cell densities of the samples (load), defined as the sample load divided by the median load over the entire MetaCardis cohort.

Multivariate effects of antibiotics and non-antibiotic drugs

The multivariate effects of antibiotics and non-antibiotic drugs on microbiome and host metabolite features were tested. Only patients and healthy individuals with complete microbiome and host metabolomic features were considered. Variables with less than 10 nonzero occurrences were excluded. In addition, variables were checked for high association using Kendall's Tau correlation for correlations

between pairs of numerical variables, intraclass correlation coefficient (ICC) for pairs of numerical versus categorical variables, and Cramer's V for pairs of categorical variables. The variables "PPI and related drugs" and "TRIMETHOPRIM" were removed from downstream analysis due to their high association (> 0.8 correlation) with other variables. The threshold of 0.8 was chosen as standard in the field^{12,48}. Finally, non-antibiotic drugs and antibiotics to be tested were selected for each microbiome feature set as well as for the set of host phenotype measurements. This was achieved by automatic stepwise model building in both directions based on the Akaike information criterion (AIC), using the function `ordistep` in `vegan` package (v2.4-5). The function chooses a model by permutation tests under constrained ordination, in this case, distance-based redundancy analysis (dbRDA) constructed on Bray-Curtis dissimilarities of square-root transformed values from each feature set. The variables selected were added to the set of control variables to compose the full models for each feature set. The control variables were selected based on their potential confounding effects. Those were BMI, sex, age, country of recruitment, stool consistency (Bristol scale), alternative healthy eating index (aHEI; as a measure of diet quality), smoking status, and patient group (i.e., disease categories or control status).

The unique effect of a given variable was assessed considering all other variables present in the model specific to each feature set. As in the model selection stage, dbRDA was constructed on Bray-Curtis dissimilarities of square-root transformed values from each feature set. The proportion of variation explained by a given variable independent of the other variables was obtained using the `Condition` function of the dbRDA implementation in the `vegan` R package (v2.4-5). For each variable of interest, a new model was constructed by including all other variables within the `Condition` function. Type III ANOVA was used to test significance of models with 999 permutations. P-values were corrected for multiple testing using the Benjamini-Hochberg procedure. Adjusted P-values below 0.05 were considered significant. Adjusted R-squared was recovered from the function using the `vegan` R function `RsquareAdj`. Adjusted R-squared was also obtained from the full model, i.e., the model constructed without the `Condition` function. All calculations were performed in the R environment v3.4.3 using the `vegan` package v 2.4-5. The code for multivariate analysis is documented and available under <https://doi.org/10.5281/zenodo.4719526>.

Univariate effects of antibiotics and non-antibiotic drugs

To assess relative roles of drugs versus disease influence on each microbiome or host measurement separately, a software pipeline was established following the approach outlined in Extended Data Figure 1. The approach followed hinges on filtering each naïve association by the outcomes of post-hoc tests for the influence of each salient covariate. In a first step, all tested features (separately by feature space, e.g. serum metabolites or gut microbial species) are checked for associations both for all group comparisons (i.e., controls versus each patient group for a case-control study like MetaCardis) and for each potential covariate, e.g. medicated versus unmedicated subjects for each drug or drug combination. This test is a two-sided Mann-Whitney U test for binary variables, Kruskal-Wallis test for other categorical variables, or a Spearman test for continuous variables. These tests are adjusted for multiple testing using Benjamini-Hochberg correction, with standardized effect sizes computed for binary variables using the Cliff's Delta metric (as implemented in the `orddom` R package (v3.1)) and Spearman's Rho for continuous variables. These tests are conducted stratified for patient groups, separate for each, for every continuous non-constant variable and every binary variable where at least 10 subjects in a patient group fall within each level of the variable. For the variable "study center", which is the one nonbinary categorical variable tested, we performed the tests in every case. For each (continuous) feature, if a covariate is significant ($FDR < 0.1$) and relevant (absolute standardized effect size > 0.1 , requirement omitted for study center) in at least one patient group, then it is tested for in the post-hoc test for all patient groups. The post-hoc test is a nested linear model comparison test, where the feature, rank-transformed, is modeled using either both the tested variable (e.g., drug or disease group comparison) and each other covariate in turn, versus a model containing only the covariate. The inverse test is also performed, comparing the more complex model to the one containing only the tested variable. P-values for these models are computed using a likelihood ratio test for the models using the R `lmtree` package (v0.9-38). If the model for the tested variable always retains significantly (post-hoc $P < 0.05$) better fit than covariate-only model omitting it, or if no salient covariates exist, the feature is considered associated under confident deconfounding with regards to the tested variable. If one or more covariates exist for which including the tested variable in the model does not significantly improve the model fit, but that the same condition holds inversely for all such covariates, then the tested feature co-occurs so

strongly with each salient covariate that it is not possible to assess whether the observed effect stems from the tested feature or the covariate; such a feature is considered ambiguously associated both with the tested variable and the covariates. Note also that it is possible for a feature to be associated even under confident deconfounding with several tested variables/covariates. If for a given feature, its dependence on a tested variable is reducible to at least one covariate that in turn cannot be reduced to the influence of the tested variable, the effect of the tested variable on the feature is considered confounded by all such features. This classification thus results in a set of feature-variable associations either confidently or ambiguously deconfounded, and in a similar map of the deconfounded associations of each possible covariate, tested separately in each patient group in MetaCardis where a naïve effect can be observed and tested. Note that “confidently deconfounded” can only be stated within the scope of available metadata.

Hierarchical clustering of drug associations with the host and microbiome features: Number of features of specific type affected by each drug falling into each category was used to cluster the drug effects. Pearson’s correlation was used as a distance metric for clustering.

Enrichment of oral strain populations in faecal samples

To quantify the differential fecal enrichment of oral strain populations, we relied on the multi-site metagenomic dataset provided by the Human Microbiome Project (HMP) to define predominantly oral microbial single nucleotide variants (SNV). Raw sequence reads for 399 stool and 945 oral HMP samples (from 9 distinct sub-sites) were downloaded from the European Nucleotide Archive (ENA: PRJNA48479, PRJNA275349), quality trimmed and mapped to reference genomes of 1,753 *speI* clusters⁴⁴ using NGlessR⁴⁶ (v1.3.0). Uniquely mapping reads for all oral sub-sites were then combined per subject and time point into a total of 375 oral samples, using the ‘samtools merge’ command. Faecal samples for the present cohort were likewise processed and mapped to the same set of *speI* reference genomes.

For the resulting combined dataset, microbial SNVs were called using metaSNV⁴⁹ (v1), requiring a minimum of 4 non-reference reads at a prevalence of $\geq 5\%$ of total samples to define an SNV. From the resulting set, all SNVs observed in at least half of oral HMP samples and at least 10 HMP fecal samples

were defined as predominantly oral and used as proxies to quantify oral microbial strain populations in MetaCardis faecal samples. By using the threshold on the lowest number of fecal samples (at least 10), we selected strains that are predominantly linked to the oral cavity, but which at least sometimes can be observed in the gut as well, which allowed us to make the test more conservative and ensure robustness to noise.

Medication intake and co-prescription frequency

To infer association rules for drug co-prescription rules, the Equivalence Class Transformation (ECLAT) algorithm implemented in the R library `arules`⁵⁰ (v 1.6-2) was used. Drug effects against disease were calculated as per the univariate tests described above; effects having the opposite direction to that found comparing patients versus controls were considered as putative drug effects, whereas effects having the same sign as the disease signature were putatively labeled as severity markers or indications for receiving a drug for purposes of visualization. Plots were generated using `ggplot2`, `ggpubr` and `igraph` R libraries, using R version 3.5.3.

Mediation analysis

To assess whether drug effects on the host features were mediated by changes in the microbiome features or vice versa, we performed general mediation analysis⁵¹ implemented in the Python (v3.7.7) library `statsmodels`⁵² (v0.11.0). For each drug or drug combination, we included only host and microbiome features that were associated with the treatment with the single drug, drug dosage or the drug combination, correspondingly. The thresholds for association were 1) MWU FDR < 0.1, 2) passing all confounder filters, 3) disease association is opposite in direction to that of the drug combination and 4) in case of dosage and combination, significance in a nested linear model comparison test (likelihood ratio post-hoc $P < 0.05$). The basic mediation analysis was performed using the formulas “feature ~ drug + mediator” for the outcome model (defined with the function `sm.GLM.from_formula`) and “mediator ~ drug” for the mediator model (defined with a function `sm.OLS.from_formula`). The effect size and significance of mediation was calculated with the function `statsmodels.stats.mediation.Mediation.fit()`

using “drug” and “mediator” as parameters. In addition to mediation analysis, we also calculated Pearson’s correlation between each feature and each mediator included in the analysis for each effector.

Acknowledgements

We thank the MetaCardis subjects for their participation in the study, and particularly the patient associations (Alliance du Coeur and CNAO) for their input and interface. We further thank Dr. Dominique Bonnefont-Rousselot (Department of Metabolic Biochemistry, Pitié-Salpêtrière hospital) for the analysis of plasma lipid profiles. We thank the nurses, technicians, clinical research assistants and data managers from the Clinical Investigation Platform at the Institute of Cardiometabolism and Nutrition for patient investigations, the Clinical Investigation Center (CIC) from Pitié-Salpêtrière Hospital and Human Research Center on Nutrition (CRNH Ile de France) as well as the university hospital of Leipzig for investigation of healthy controls. Quanta Medical provided regulatory oversight of the clinical study and contributed to the processing and management of electronic data.

Availability of data and materials

The source data for the figures and corresponding code are provided under <https://doi.org/10.5281/zenodo.4728981>. Raw shotgun sequencing data that support the findings of this study have been deposited in The European Nucleotide Archive (ENA) with accession codes [PRJEB41311, PRJEB38742 and PRJEB37249] with public access. Raw spectra for metabolomics have been deposited in the MassIVE database under the accession codes [UPLC-MS/MS] MSV000088043 and [GCMS] MSV000088042. The metadata on disease groups and drug intake are provided in Supplementary Tables 1, 2 and 3. The demographic, clinical and phenotype metadata for French and German participants, and processed microbiome and metabolome data for French, German and Danish participants are available under <https://doi.org/10.5281/zenodo.4674360> for download. According to the Danish Data Protection Act of 2018 and Danish interpretation of European GDPR, individual pseudonymized phenotype metadata from the Danish participants in the present study cannot be reported or shared in any public scientific database unless access is granted on a case-by-case base by the Danish Data Protection Agency following prior formal application. Thus, for reasons of legal restrictions, access

to phenotype metadata from the Danish participants is controlled. To apply for access to the Danish participant phenotype metadata used in this article, please contact the corresponding author (PB), who will take the request further to the lead author responsible for the Danish participants (OP) to contact the Danish Data Protection Agency.

Code availability

The novel drug-aware univariate biomarker testing pipeline is available as an R package (metadeconfoundR; Birkner et al., manuscript in preparation) on Github (<https://github.com/TillBirkner/metadeconfoundR>) and under <https://doi.org/10.5281/zenodo.4721078>. The latest version (0.1.8) of this package was used to generate the data shown in this publication. The code used for multivariate analysis based on the VpThemAll package is available under <https://doi.org/10.5281/zenodo.4719526>. The phenotype and drug intake metadata, processed microbiome and metabolome data and code resource are available under <https://doi.org/10.5281/zenodo.4674360> for download. The source data for the figures and corresponding code are provided under <https://doi.org/10.5281/zenodo.4728981>.

Sources of funding

This work was supported by the European Union's Seventh Framework Program for research, technological development and demonstration under grant agreement HEALTH-F4-2012-305312 (METACARDIS). Part of this work was also supported by the EMBL, by the Metagenopolis grant ANR-11-DPBS-0001, by the H2020 European Research Council (ERC-AdG-669830) (to PB), and by grants from the Deutsche Forschungsgemeinschaft (SFB1365 to SKF and LM, and SFB1052/3 A1 MS to MS (Project:209933838)). Assistance Publique-Hôpitaux de Paris (AP-HP) is the promoter of the clinical investigation (MetaCardis). MED is supported by the NIHR Imperial Biomedical Research Centre. The Novo Nordisk Foundation Center for Basic Metabolic Research is an independent research institution at the University of Copenhagen partially funded by an unrestricted donation from the Novo Nordisk Foundation.

Author contributions

KC (coordinator), PB, MS, OP, SDE, JR, M-ED, FB and JN conceived the overall objectives and study design of the MetaCardis initiative. SKF, PB developed the present project concept and protocol and supervised the project. MetaCardis cohort recruitment, phenotyping and lifestyle recording were conducted by: RC, JA-W, TN, CL, LK, TH, THH, HV, KA and supervised by MS, KC and OP. Data curation was undertaken by: SKF, RC, LM, KA, JA-W, TN. Faecal microbial DNA extraction and shotgun sequencing: NP, ELC, SF. Bacterial cell count measurement: GF, SVS. Serum and urine metabolome profiling: LH, JC, AM, MO. Bioinformatics and statistical analyses: TB, MZ-K, SKF, LS, TSBS, LPC, NS, JZ, EP, SF, RC, SV, GF and BJ. The manuscript was drafted by SKF, RC, MZ-K, LM. All authors participated in the project development, revision of article and approved the final version for publication.

Competing interests

FB is shareholder in Implexion pharma AB. KC is a consultant for Danone Research, LNC therapeutics and CONFO therapeutics for work unassociated with the present study. KC has held a collaborative research contract with Danone Research in the context of MetaCardis project. MB received lecture and/or consultancy fees from AstraZeneca, Boehringer-Ingelheim, Lilly, Novo Nordisk, Novartis and Sanofi. The remaining authors do not report any competing interests.

References

1. Sinha, R. *et al.* Assessment of variation in microbial community amplicon sequencing by the Microbiome Quality Control (MBQC) project consortium. *Nature biotechnology* **35**, 1077–1086; 10.1038/nbt.3981 (2017).
2. Costea, P. I. *et al.* Towards standards for human fecal sample processing in metagenomic studies. *Nature biotechnology* **35**, 1069–1076; 10.1038/nbt.3960 (2017).
3. Rothschild, D. *et al.* Environment dominates over host genetics in shaping human gut microbiota. *Nature* **555**, 210–215; 10.1038/nature25973 (2018).
4. Schmidt, T. S. B., Raes, J. & Bork, P. The Human Gut Microbiome: From Association to Modulation. *Cell* **172**, 1198–1215; 10.1016/j.cell.2018.02.044 (2018).
5. Vujkovic-Cvijin, I. *et al.* Host variables confound gut microbiota studies of human disease. *Nature*; 10.1038/s41586-020-2881-9 (2020).
6. Tsuda, A. *et al.* Influence of Proton-Pump Inhibitors on the Luminal Microbiota in the Gastrointestinal Tract. *Clinical and translational gastroenterology* **6**, e89; 10.1038/ctg.2015.20 (2015).
7. Forslund, K. *et al.* Disentangling type 2 diabetes and metformin treatment signatures in the human gut microbiota. *Nature* **528**, 262–266; 10.1038/nature15766 (2015).
8. Maier, L. *et al.* Extensive impact of non-antibiotic drugs on human gut bacteria. *Nature* **555**, 623–628; 10.1038/nature25979 (2018).
9. Le Bastard, Q. *et al.* Systematic review: human gut dysbiosis induced by non-antibiotic prescription medications. *Alimentary pharmacology & therapeutics* **47**, 332–345; 10.1111/apt.14451 (2018).
10. Vich Vila, A. *et al.* Impact of commonly used drugs on the composition and metabolic function of the gut microbiota. *Nature communications* **11**; 10.1038/s41467-019-14177-z (2020).
11. Vieira-Silva, S. *et al.* Statin therapy is associated with lower prevalence of gut microbiota dysbiosis. *Nature* **581**, 310–315; 10.1038/s41586-020-2269-x (2020).
12. Falony, G. *et al.* Population-level analysis of gut microbiome variation. *Science* **352**, 560–564; 10.1126/science.aad3503 (2016).
13. Jackson, M. A. *et al.* Gut microbiota associations with common diseases and prescription medications in a population-based cohort. *Nature communications* **9**, 2655; 10.1038/s41467-018-05184-7 (2018).
14. Conlon, M. A. & Bird, A. R. The impact of diet and lifestyle on gut microbiota and human health. *Nutrients* **7**, 17–44; 10.3390/nu7010017 (2014).
15. Blaser, M. J. Antibiotic use and its consequences for the normal microbiome. *Science* **352**, 544–545; 10.1126/science.aad9358 (2016).
16. Imhann, F. *et al.* Proton pump inhibitors affect the gut microbiome. *Gut* **65**, 740–748; 10.1136/gutjnl-2015-310376 (2016).
17. Imhann, F. *et al.* The influence of proton pump inhibitors and other commonly used medication on the gut microbiota. *Gut Microbes* **8**, 351–358; 10.1080/19490976.2017.1284732 (2017).
18. Wu, H. *et al.* Metformin alters the gut microbiome of individuals with treatment-naive type 2 diabetes, contributing to the therapeutic effects of the drug. *Nature medicine* **23**, 850–858; 10.1038/nm.4345 (2017).
19. Koeth, R. A. *et al.* γ -Butyrobetaine is a proatherogenic intermediate in gut microbial metabolism of L-carnitine to TMAO. *Cell metabolism* **20**, 799–812; 10.1016/j.cmet.2014.10.006 (2014).
20. Kopp, E. & Ghosh, S. Inhibition of NF-kappa B by sodium salicylate and aspirin. *Science* **265**, 956–959; 10.1126/science.8052854 (1994).

21. Davalli, A. M., Perego, C. & Folli, F. B. The potential role of glutamate in the current diabetes epidemic. *Acta diabetologica* **49**, 167–183; 10.1007/s00592-011-0364-z (2012).
22. Schmidt, T. S. *et al.* Extensive transmission of microbes along the gastrointestinal tract. *eLife* **8**; 10.7554/eLife.42693 (2019).
23. Shimazu, T. *et al.* Suppression of Oxidative Stress by β -Hydroxybutyrate, an Endogenous Histone Deacetylase Inhibitor. *Science* **339**, 211–214; 10.1126/science.1227166 (2012).
24. Shah, B. R. & Hux, J. E. Quantifying the risk of infectious diseases for people with diabetes. *Diabetes care* **26**, 510–513; 10.2337/diacare.26.2.510 (2003).
25. Korpela, K. & Vos, W. M. de. Antibiotic use in childhood alters the gut microbiota and predisposes to overweight. *Microbial Cell* **3**, 296–298; 10.15698/mic2016.07.514 (2016).
26. Le Chatelier, E. *et al.* Richness of human gut microbiome correlates with metabolic markers. *Nature* **500**, 541–546; 10.1038/nature12506 (2013).
27. Arumugam, M. *et al.* Enterotypes of the human gut microbiome. *Nature* **473**, 174–180; 10.1038/nature09944 (2011).
28. Costea, P. I. *et al.* Enterotypes in the landscape of gut microbial community composition. *Nature microbiology* **3**, 8–16; 10.1038/s41564-017-0072-8 (2018).
29. Cameron, A. R. *et al.* Anti-Inflammatory Effects of Metformin Irrespective of Diabetes Status. *Circulation research* **119**, 652–665; 10.1161/CIRCRESAHA.116.308445 (2016).
30. Dandona, P. *et al.* Increased plasma concentration of macrophage migration inhibitory factor (MIF) and MIF mRNA in mononuclear cells in the obese and the suppressive action of metformin. *The Journal of clinical endocrinology and metabolism* **89**, 5043–5047; 10.1210/jc.2004-0436 (2004).

**** MetaCardis Consortium Collaborators**

Chloe Amouyal ^{7, 26}, Ehm Astrid Andersson Galijatovic ⁹, Fabrizio Andreelli ^{7, 8, 26}, Olivier Barthelemy ¹⁸, Jean-Paul Batisse ¹⁸, Eugeni Belda ²⁰, Magalie Berland ¹⁷, Randa Bittar ³³, Hervé Blottière ¹⁷, Frederic Bosquet ²⁶, Rachid Boubrit ¹⁸, Olivier Bourron ²⁶, Mickael Camus ¹⁷, Dominique Cassuto ⁸, Cecile Ciangura ^{8, 26}, Jean-Philippe Collet ¹⁸, Maria-Carlota Dao ⁷, Morad Djebbar ¹⁸, Angélique Doré ¹⁷, Line Engelbrechtsen ⁷, Soraya Fellahi ^{11, 12}, Sebastien Fromentin ¹⁷, Pilar Galan ¹⁴, Dominique Gauguier ^{38, 29}, Philippe Giral ³⁴, Agnes Hartemann ²⁶, Bolette Hartmann ⁹, Jens Juul Holst ⁹, Malene Hornbak ⁹, Lesley Hoyles ³², Jean-Sebastien Hulot ^{22, 35, 36}, Sophie Jaqueminet ¹⁷, Niklas Rye Jørgensen ²⁴, Hanna Julienne ¹⁷, Johanne Justesen ⁹, Judith Kammer ⁶, Nikolaj Krarup ⁹, Mathieu Kerneis ¹⁸, Jean Khemis ⁸, Ruby Kozlowski ¹⁴, Véronique Lejard ¹⁷, Florence Levenez ¹⁷, Lea Lucas-Martini ⁸, Robin Massey ¹⁷, Laura Martinez-Gili ¹⁴, Nicolas Maziers ¹⁷, Jonathan Medina-Stamminger ⁸, Gilles Montalescot ¹⁸, Sandrine Moute ²¹, Ana Luisa Neves ¹⁴, Michael Olanipekun ^{14, 27}, Laetitia Pasero Le Pavin ¹⁷, Christine Poitou ^{7, 8}, Françoise Pousset ¹⁸, Laurence Pouzoulet ³⁴, Andrea Rodriguez-Martinez ¹⁴, Christine Rouault ⁷, Johanne Silvain ¹⁸, Mathilde Svendstrup ⁹, Timothy Swartz ^{7, 20, 37}, Thierry Vanduyvenboden ¹⁷, Camille Vatiez ⁸, Stefanie Walther ⁶

- 32 Department of Biosciences, Nottingham Trent University, Nottingham, UK
- 33 Assistance Publique Hôpitaux de Paris, Pitie-Salpêtrière Hospital, Biochemistry Department of Metabolic Disorders, Paris, France.
- 34 Assistance Publique Hôpitaux de Paris, Endocrinology Department, Pitie-Salpêtrière Hospital, Paris, France.
- 35 PARCC, INSERM, Université de Paris, Paris, France.
- 36 Assistance Publique Hôpitaux de Paris, Hôpital Européen Georges-Pompidou, CIC1418 and DMU CARTE, Paris, France.
- 37 Integrative Phenomics, Paris, France.
- 38 UMRS 1124 INSERM, Université de Paris Descartes, Paris, France

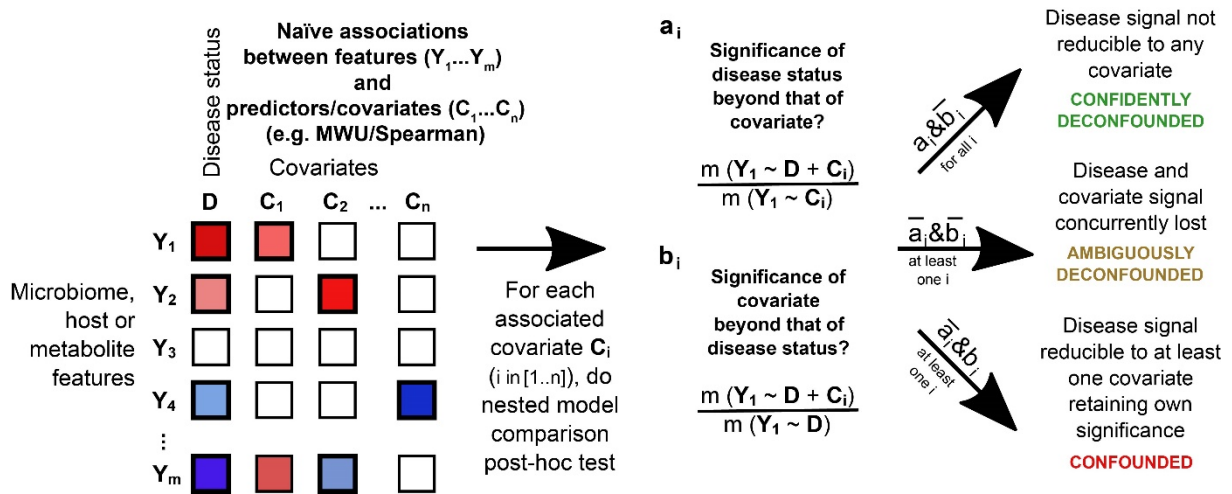
Methods References

31. Palleja, A. *et al.* Recovery of gut microbiota of healthy adults following antibiotic exposure. *Nature microbiology* **3**, 1255–1265; 10.1038/s41564-018-0257-9 (2018).
32. Prest, E. I., Hammes, F., Köttsch, S., van Loosdrecht, M. C. M. & Vrouwenvelder, J. S. Monitoring microbiological changes in drinking water systems using a fast and reproducible flow cytometric method. *Water research* **47**, 7131–7142; 10.1016/j.watres.2013.07.051 (2013).
33. Branca, F., Nikogosian, H. & Lobstein, T. The challenge of obesity in the WHO European Region and the strategies for response. Summary. Available at <https://www.euro.who.int/en/publications/abstracts/challenge-of-obesity-in-the-who-european-region-and-the-strategies-for-response-the.-summary>.
34. Alberti, K. G. M. M., Zimmet, P. & Shaw, J. The metabolic syndrome - a new worldwide definition. *Lancet (London, England)* **366**, 1059–1062; 10.1016/S0140-6736(05)67402-8 (2005).
35. Petersmann, A. *et al.* Definition, Classification and Diagnosis of Diabetes Mellitus. *Experimental and clinical endocrinology & diabetes: official journal, German Society of Endocrinology and German Diabetes Association* **127**, S1-S7; 10.1055/a-1018-9078 (2019).
36. Whelton, P. K. *et al.* 2017 ACC/AHA/AAPA/ABC/ACPM/AGS/APhA/ASH/ASPC/NMA/PCNA Guideline for the Prevention, Detection, Evaluation, and Management of High Blood Pressure in Adults: Executive Summary: A Report of the American College of Cardiology/American Heart Association Task Force on Clinical Practice Guidelines. *Hypertension (Dallas, Tex.: 1979)* **71**, 1269–1324; 10.1161/HYP.000000000000066 (2018).
37. Yancy, C. W. *et al.* 2017 ACC/AHA/HFSA Focused Update of the 2013 ACCF/AHA Guideline for the Management of Heart Failure: A Report of the American College of Cardiology/American Heart Association Task Force on Clinical Practice Guidelines and the Heart Failure Society of America. *Journal of cardiac failure* **23**, 628–651; 10.1016/j.cardfail.2017.04.014 (2017).
38. Verger, E. O. *et al.* Dietary Assessment in the MetaCardis Study: Development and Relative Validity of an Online Food Frequency Questionnaire. *Journal of the Academy of Nutrition and Dietetics* **117**, 878–888; 10.1016/j.jand.2016.10.030 (2017).

39. Criscuolo, A. & Brisse, S. AlienTrimmer: a tool to quickly and accurately trim off multiple short contaminant sequences from high-throughput sequencing reads. *Genomics* **102**, 500–506; 10.1016/j.ygeno.2013.07.011 (2013).
40. Li, J. *et al.* An integrated catalog of reference genes in the human gut microbiome. *Nature biotechnology* **32**, 834–841; 10.1038/nbt.2942 (2014).
41. Cotillard, A. *et al.* Dietary intervention impact on gut microbial gene richness. *Nature* **500**, 585–588; 10.1038/nature12480 (2013).
42. Prifti, E. & Le Chatelier, E. MetaOMineR. a quantitative metagenomics data analyses pipeline. (hal-02800484) (2014).
43. Nielsen, H. B. *et al.* Identification and assembly of genomes and genetic elements in complex metagenomic samples without using reference genomes. *Nature biotechnology* **32**, 822–828; 10.1038/nbt.2939 (2014).
44. Sunagawa, S. *et al.* Metagenomic species profiling using universal phylogenetic marker genes. *Nature methods* **10**, 1196–1199; 10.1038/nmeth.2693 (2013).
45. Kultima, J. R. *et al.* MOCAT2: a metagenomic assembly, annotation and profiling framework. *Bioinformatics* **32**, 2520–2523; 10.1093/bioinformatics/btw183 (2016).
46. Coelho, L. P. *et al.* NG-meta-profiler: fast processing of metagenomes using NGLess, a domain-specific language. *Microbiome* **7**, 84; 10.1186/s40168-019-0684-8 (2019).
47. Vandeputte, D. *et al.* Quantitative microbiome profiling links gut community variation to microbial load. *Nature* **551**, 507–511; 10.1038/nature24460 (2017).
48. Katz, M. H. *Multivariable Analysis. A Practical Guide for Clinicians and Public Health Researchers.* Cambridge University Press, Cambridge, (2011).
49. Costea, P. I. *et al.* metaSNV: A tool for metagenomic strain level analysis. *PloS one* **12**, e0182392; 10.1371/journal.pone.0182392 (2017).
50. Hahsler M., Gruen B., Hornik K. arules – A Computational Environment for Mining Association Rules and Frequent Item Sets. *Journal of Statistical Software*, 14(15), 1–25. (2005).
51. Imai, K., Keele, L. & Tingley, D. A general approach to causal mediation analysis. *Psychological methods* **15**, 309–334; 10.1037/a0020761 (2010).
52. Seabold, S. & Perktold J. statsmodels: Econometric and Statistical Modeling with Python. *9th Python in Science Conference* (2010).
53. Le Chatelier, E. *et al.* Richness of human gut microbiome correlates with metabolic markers. *Nature* **500**, 541–546; 10.1038/nature12506 (2013).
54. Cani, P. D. *et al.* Metabolic endotoxemia initiates obesity and insulin resistance. *Diabetes* **56**, 1761–1772; 10.2337/db06-1491 (2007).

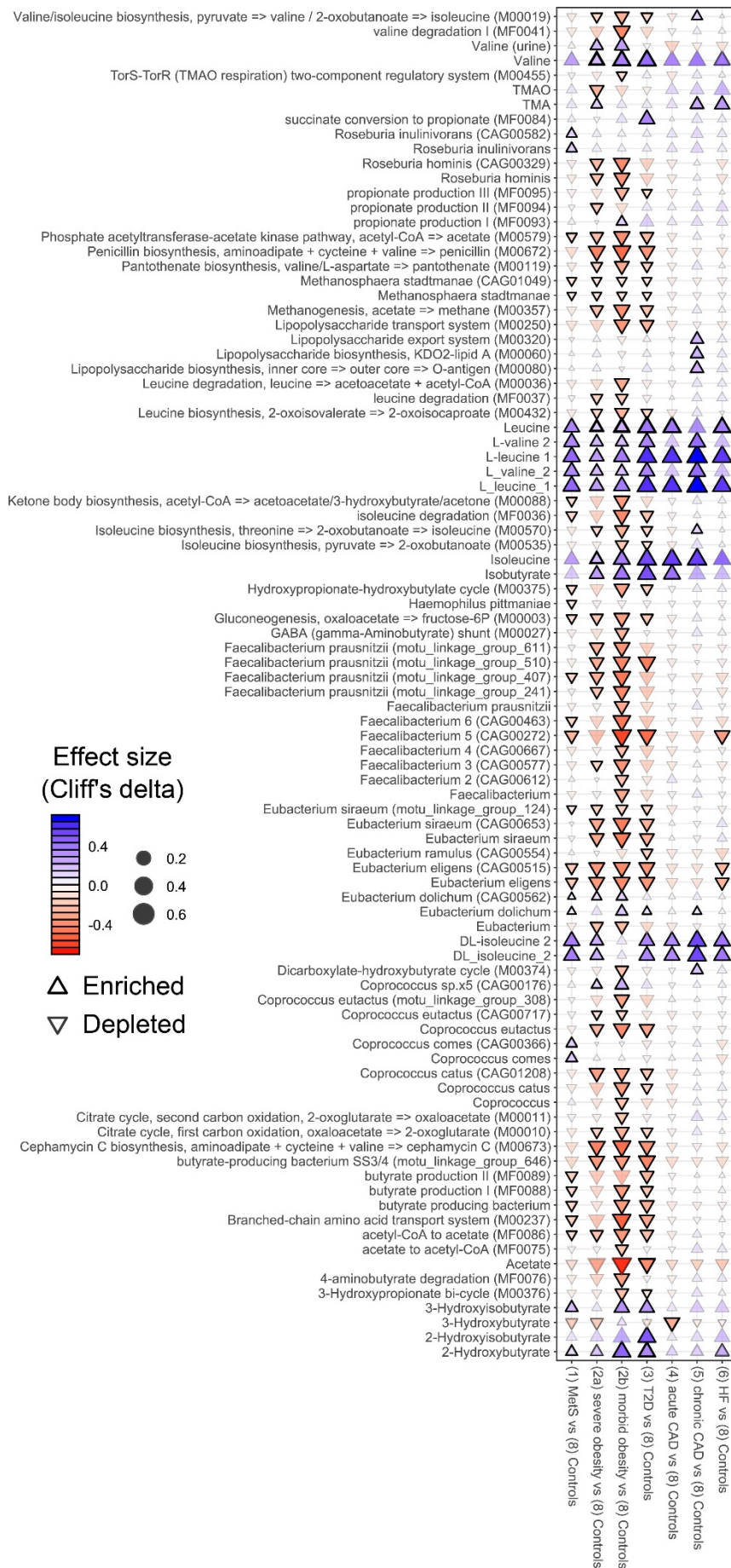
Extended Data Figures

ED Figure 1.



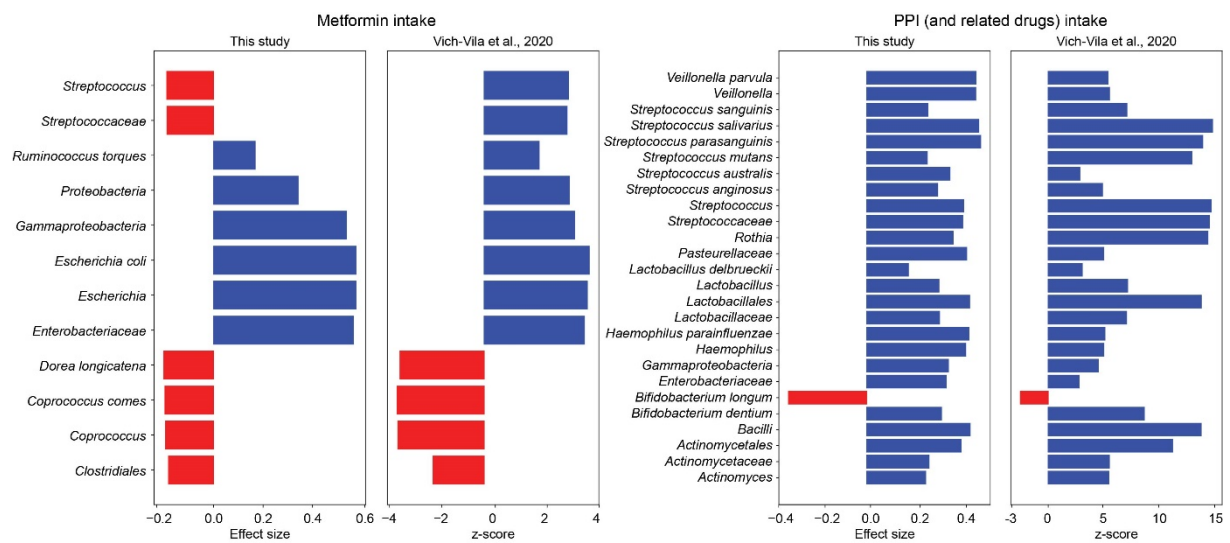
ED Figure 1. A post-hoc testing approach for deconfounding univariate biomarker analysis for multiple medications and risk factors. The schematic highlights our covariate control approach. All significant associations between putative drivers (e.g., disease D) and covariates ($C_1 \dots C_n$) to each measured feature ($Y_1 \dots Y_m$) are taken. The outcome of the test is denoted with a_i for a positive outcome (“yes”) and \bar{a}_i for a negative outcome (“no”). A significant predictor is called “confounded” and is filtered out in a post-hoc test if there is at least one covariate (e.g., drug treatment or combination) such that the predictor does not add significant predictive capacity beyond the covariate (“confounded”). If no such covariate itself passes the same test (i.e., covariates cannot in turn be shown to have predictive capacity beyond tested predictor), the predictor is considered ambiguous (“ambiguously deconfounded”). Otherwise, the predictor is considered “confidently deconfounded” (we note that “confidently deconfounded” is defined as no confounders were found among all covariates measured in our study).

ED Figure 2.



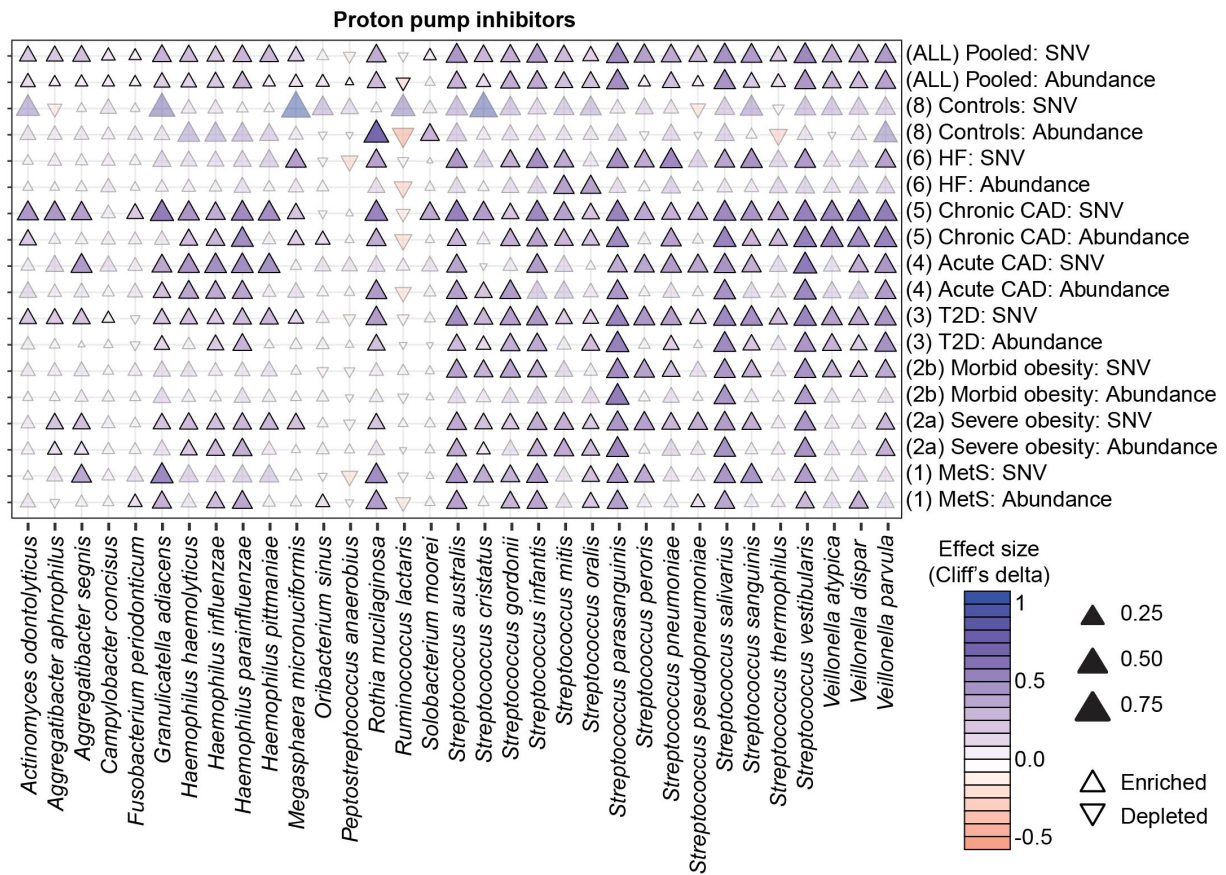
ED Figure 2. Previously reported metabolic disease associations are replicated in the MetaCardis cohort under drug deconfounding, highlighting systemic inflammation, short-chain fatty acid and branched-chain amino acid mechanisms underlying insulin resistance. Cuneiform plot marker hues and direction show sign of effect size (Cliff's delta), intensity and size show amplitude of effect size, comparing metabolic diseased proband subsets (horizontal axis) with healthy control subject in the MetaCardis population for different microbiome, metabolome and host features (vertical axis). Bold and opaque markers show significant associations (two-sided MWU FDR < 0.1) not reducible to any significant drug or demographic confounder. Full associations are found in Supplementary Table 9; here a preselected subset is displayed reflecting previously reported risk and protective factors, validated in MetaCardis. ¹H NMR features are shown with retention time in parentheses, functional modules with GMM or KEGG identifier in parenthesis, analogous for metagenomic species and mOTUs.

ED Figure 3.



ED Figure 3. Previously reported drug-microbiome associations are replicated in the MetaCardis cohort for metformin and PPI. Bar plots show the magnitude and direction of effect size (Cliff's delta) of metformin treatment (left) and PPI treatment (right) on microbiome features. These effects are compared to the previously published data from two independent patient cohorts¹⁰. Only features with direct match on the taxonomic level were included in the comparison. Full list of associations is provided in Supplementary Table 6.

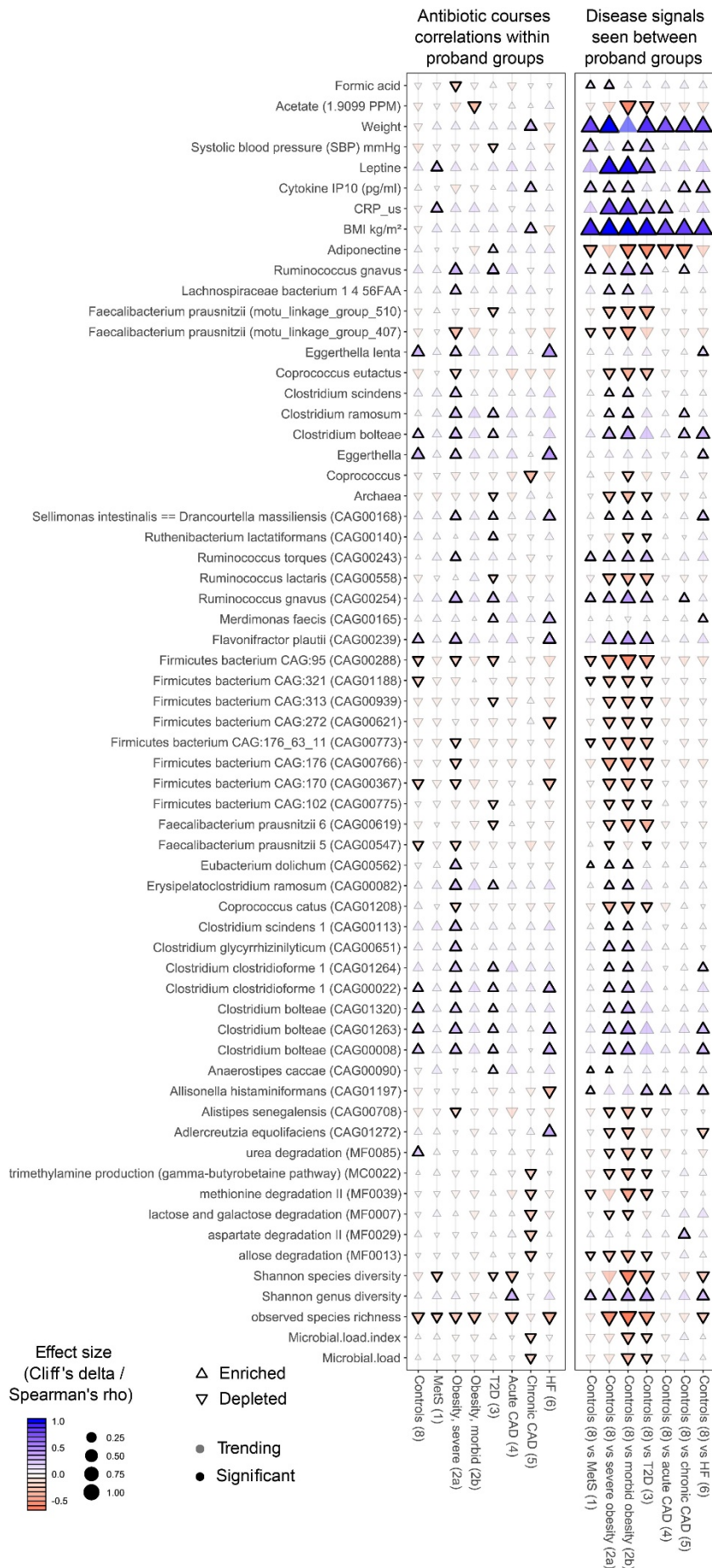
ED Figure 4.



ED Figure 4. Single nucleotide variation analysis of strains in the gut of subjects taking PPIs.

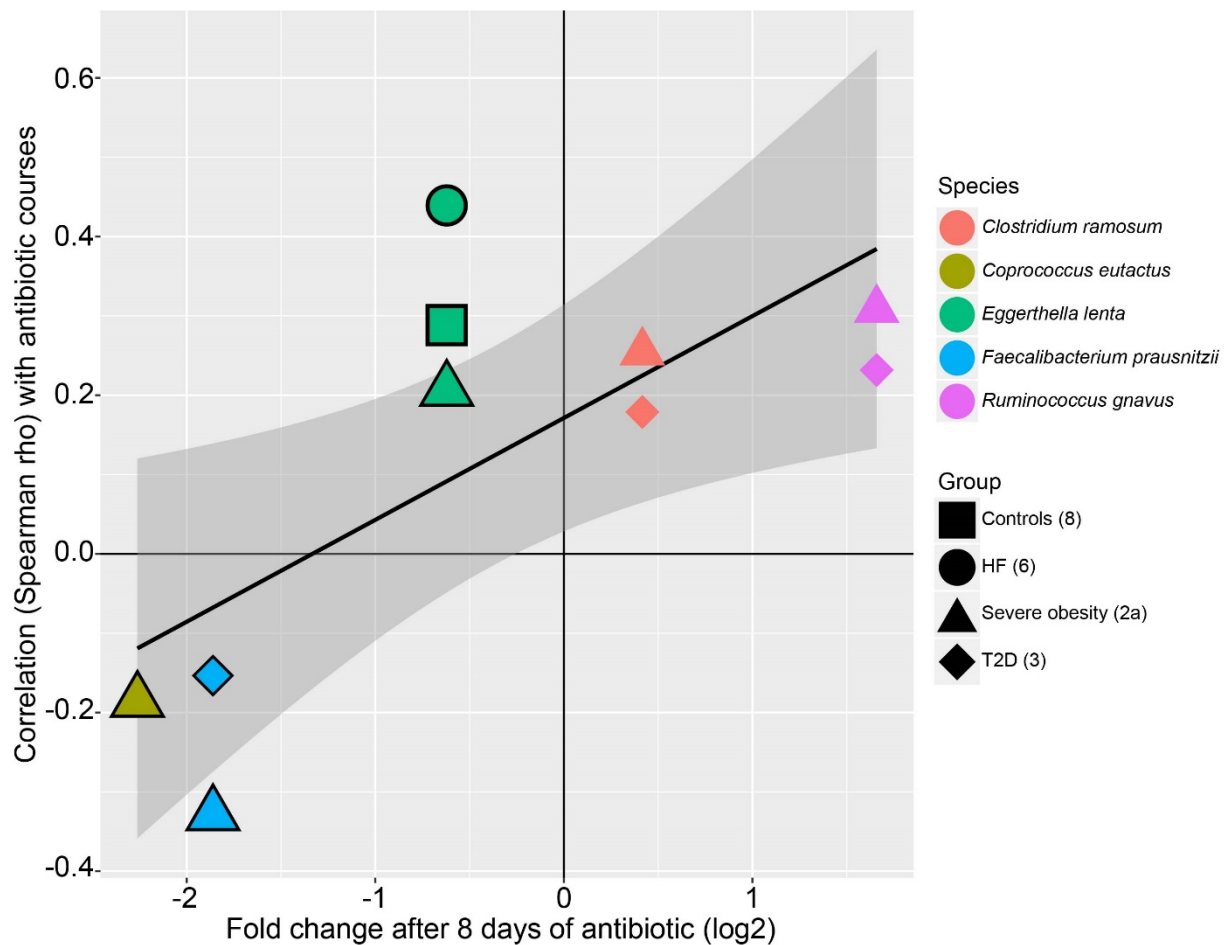
Cuneiform plot shows change in abundance of bacterial species in the gut in subjects taking/not taking PPIs (controlling for other drugs and demographic factors) in each clinical group separately, and for all subjects pooled together. Rows marked “SNV” show whether oral strain single nucleotide markers are significantly (two-sided MWU FDR < 0.1) enriched over gut strain markers in subjects taking PPIs, controlling for abundance of each species. Marker direction, color and size denote the sign and value of Cliff’s delta standardized effect size; opaque markers are significantly altered (two-sided MWU FDR < 0.1; passing all confounder checks). Bacteria are shown if their abundance is significantly altered under PPI consumption, and there are SNPs distinguishing oral from gut strains in HMP samples. (See Supplementary Tables 5-7).

ED Figure 5.



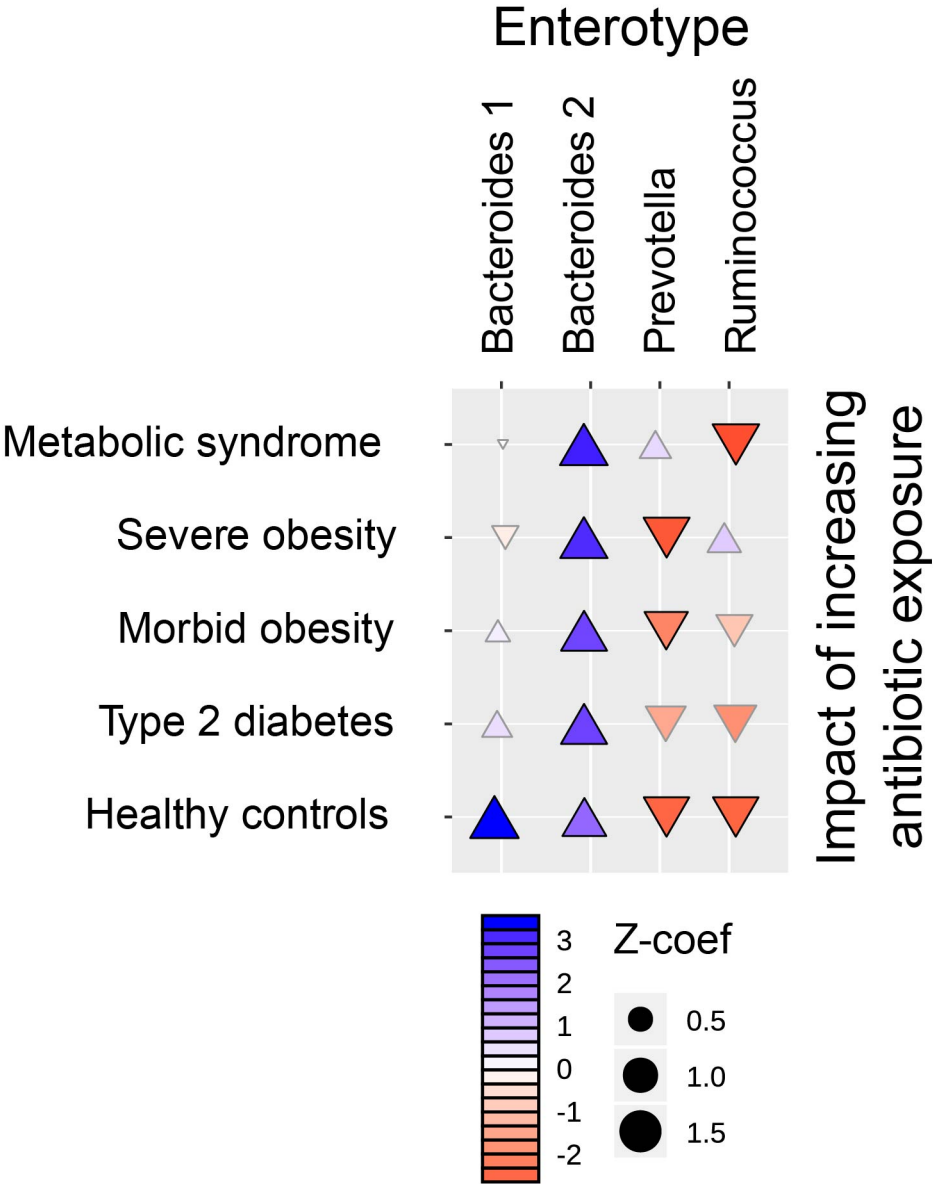
ED Figure 5. Breakdown of antibiotics association into individual features, selected features shown. Left cuneiform plot (markers show Spearman correlation direction by shape and color, scope by size and color, significance (two-sided MWU FDR < 0.1, deconfounded for other drug and demographic features) by edge opacity) shows association between each feature and total number of antibiotics courses in CMD groups as well as in healthy controls. Right cuneiform shows whether the same features are significantly different (two-sided MWU FDR < 0.1) between healthy controls and CMD subjects following drug deconfounding (markers show Cliff's delta effect size), requiring significant and deconfounded correlation with number of antibiotic courses demonstrable in at least one proband group and at least one group showing significant and deconfounded alteration compared to healthy controls. Core features include increased carriage of possible disease-associated *Ruminococcus gnavus* and various *Clostridia* species, alongside decreased carriage of commensals such as *Faecalibacterium* species. Full list of associations is provided in Supplementary Table 12.

ED Figure 6.



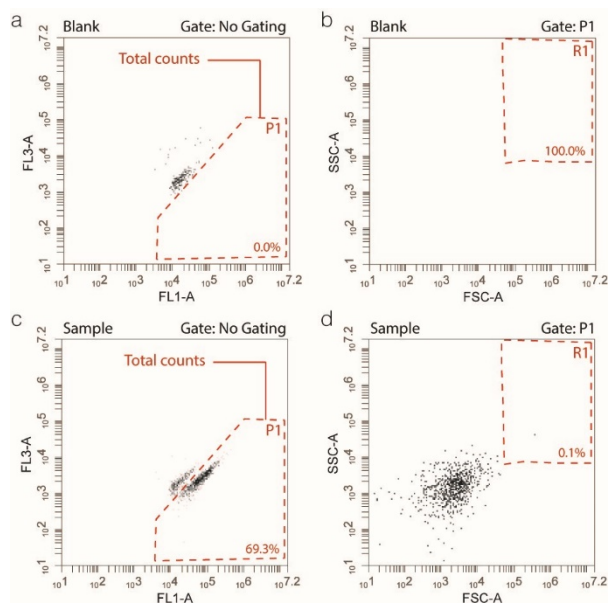
ED Figure 6. Taxonomic changes are validated in a recent intervention cohort. For bacterial species where an effect on abundance of total antibiotics courses in MetaCardis could be demonstrated (significant at Spearman FDR < 0.1 and deconfounded), where effect of antibiotic intervention could also be tested in a recent antibiotic intervention study³¹, effect sizes are shown here (MetaCardis correlation on vertical axis, intervention log-transformed fold change on horizontal axis). Separate markers are shown for each MetaCardis patient group within which antibiotic effect can be demonstrated. Bold markers achieve significance (FDR < 0.1) in the intervention study as well. For the majority of taxa overlapping between studies, direction of changes matches, consistent with a causal impact of antibiotics on the microbiota in MetaCardis.

ED Figure 7.



ED Figure 7. Enterotype likelihood is altered by antibiotics. Cuneiform shows normalized regression coefficients of logistic models for each 4-class enterotype as a function of antibiotics courses in the last 5 years, separately for controls and metabolic disease patient groups. All significant (two-sided Wald FDR < 0.1) models show depletion of Ruminococcus and Prevotella enterotypes, and enrichment for Bacteroides enterotypes; in the case of metabolic disease patients, this is strongest for the low cell count Bacteroides 2 enterotype.

ED Figure 8.



ED Figure 8. Illustration of flow cytometry gating strategy. A fixed gating/staining approach was applied³². Both blank and sample solutions were stained with SYBR Green I.

a. FL1-A/FL3-A acquisition plot of a blank sample (0.85% w/v physiological solution) with gate boundaries indicated. A threshold value of 2000 was applied on the FL1 channel.

b. Secondary gating was performed on the FSC-A/SSC-A channels to further discriminate between debris/background and microbial events.

c, d./ FL1-A/FL3-A count acquisition of a faecal sample with secondary gating on FSC-A/SSC-A channels based on blank analyses. Total counts were defined as events registered in the FL1-A/FL3-A gating area excluding debris/background events observed in the FSC-A/SSC-A R1 gate. The flow rate was set at 14 microliters per minute and the acquisition rate did not exceed 10,000 events per second. Each panel reflects the events registered during a 30 seconds acquisition period. Cell counts were determined in duplicate starting from a single biological sample.